Characterization of Matrix Metalloproteinase-8 (MMP-8) Structure and Stability and the Effects of Its Interaction with the Inhibitory Metal Abstraction Peptide NCC Using High-Resolution Solution NMR

By

Alana M. Schlemmer

Submitted to the graduate degree program in Chemistry and the Graduate Faculty of the University of Kansas in partial fulfillment of the requirements for the degree of Master of Science.

_____

Chairperson/Cindy L. Berrie, Ph.D.

_____

Paulette Spencer, Ph.D., D.D.S.

_____

Roberto N. De Guzman, Ph.D.

_____

Michael A. Johnson, Ph.D.

Date Defended: July 27, 2016

The Thesis Committee for Alana M. Schlemmer certifies that
this is the approved version of the following thesis:

Characterization of Matrix Metalloproteinase-8 (MMP-8) Structure and Stability and the Effects of Its Interaction with the Inhibitory Metal Abstraction Peptide NCC Using High-Resolution Solution NMR

_____

Chairperson/Cindy L. Berrie, Ph.D.

Date Approved: July 27, 2016

ABSTRACT

Matrix metalloproteinases (MMPs) are important enzymes for extracellular matrix degradation. Cleavage of collagen by MMP-8 is an important regulator of tissue remodeling in wound healing and repair, but it also contributes to the exacerbation of several inflammatory diseases and can serve a protective role in early stages of cancer. In addition through its enzymatic activity, MMP-8 directly effects disease progression through up-regulation or down-regulation of key inflammatory mediators and proteins involved in tissue repair, neutrophil migration, and inflammation. As such, MMP-8 has been a therapeutic target for inhibition with the aim to improve patient care and outcomes for several inflammatory diseases, such as periodontitis, asthma, and rheumatoid arthritis. Several MMP-8 inhibitors have been investigated, but often, the mechanisms of inhibition are not fully understood. To better understand MMP-8 inhibition, high-resolution solution nuclear magnetic resonance (NMR) spectroscopy has been used to study protein structure under different conditions and to track perturbations from inhibitor interactions. Knowing the mechanism of inhibitor interaction would allow for the development of more selective and potent MMP-8 inhibitors. The primary objectives of this thesis are to give an overview of the mechanistic action of MMP-8 in the immune response, to understand the structure and behavior of MMP-8 in various conditions using NMR spectroscopy, and to explore interaction of this enzyme with the unique metal abstraction peptide (MAP) inhibitor NCC.

ACKNOWLEDGEMENTS

The research described in this dissertation was conceived by and performed under the advisement of Dr. Jennifer Laurence in the Department of Pharmaceutical Chemistry. The work was supported by the NIH/NIDCR Grant No. R01-DE022054 and Collaborative Administrative Supplement DE022054-04S1 and by the Department of Chemistry at the University of Kansas.

The success of this work was possible through the assistance of others within the KU community. This work made use of the KU Biomolecular NMR Core Facility, and I would like to thank Drs. Justin Douglas and Asokan Anabanadam for their training and assistance on the NMR spectrometers and NMR data processing and analysis. I would also like to thank Dr. Roberto De Guzman for assistance with NMR data processing and analysis. I would like to thank current and former members of the Laurence lab for their training, assistance, and encouragement during my graduate career. I would especially like the thank Michaela McNiff for her training and assistance throughout my time as a graduate student. I would also like to thank my committee (Drs. Cindy Berrie, Paulette Spencer, Roberto De Guzman, and Michael Johnson) for serving on my committee and for offering advice to improve my research.

I would like to thank my family and friends for their support during my graduate career. My husband, Zac, was a great listener as I would often talk to him about my research, and he provided constant encouragement throughout my time as a graduate student. He understood the demands of graduate school and helped to relieve my stress and offer advice when my projects were not working correctly. My parents and brother constantly supported and encouraged me, even though they may not have fully understood my research projects. My husband, family, and friends helped to keep me motivated as I worked to get my degree.

I would like to thank Drs. Jennifer Laurence and Paulette Spencer for providing support of my research. Finally, I would like to thank my advisor, Dr. Jennifer Laurence, for taking me into her lab group, even though I was not in her department. I really appreciate her mentorship and helpful discussion which challenged me and helped me think critically and grow as a scientist. I am very thankful for all of her support on both a personal and professional level.

CONFLICT OF INTEREST STATEMENT

JENNIFER S. LAURENCE IS THE CO-OWNER OF ECHOGEN INC., A LIMITED LIABILITY COMPANY THAT HAS LICENSED THE PATENT-PROTECTED METAL ABSTRACTION PEPTIDE (MAP) TECHNOLOGY, ON WHICH THE *claMP* TAG IS BASED, FROM THE UNIVERSITY OF KANSAS. ALL STUDIES WERE PERFORMED AND PRESENTATION OF RESULTS PRESENTED IN ACCORDANCE WITH THE TERMS OF THE LICENSE AGREEMENT BETWEEN ECHOGEN AND KANSAS UNIVERSITY.

TABLE OF CONTENTS

LIST OF FIGURES

LIST OF ABBREVIATIONS

In alphabetical order:

2D	Two-dimensional
3D	Three-dimensional
AEMA	2-Aminoethyl methacrylate hydrochloride
CAPE	Caffeic acid phenethyl ester
CD	Circular dichroism
CHX	Chlorohexidine
COPD	Chronic obstructive pulmonary disease
CV	Column volumes
DEX	Dexamethasone
DMSO	Dimethyl sulfoxide
E. coli	*Escherichia coli*
ELISA	Enzyme-linked immunosorbent assay
GCF	Gingival crevicular fluid
HPdLF	Human periodontal ligament fibroblast
HSQC	Heteronuclear single quantum coherence
IFMA	Immunofluorometric assay
IL	Interleukin
ILV	Isoleucine, leucine, valine
IP	Interferon-γ inducible protein
IPTG	Isopropyl β-D-1-thiogalactopyranoside
LIX	Lipopolysaccharide-induced CXC chemokine

MAP	Metal abstraction peptide
MIP	Macrophage inflammatory protein
mMMP	Mouse matrix metalloproteinase
MMP	Matrix metalloproteinase
MW	Molecular weight
MWCO	Molecular weight cut-off
Nb	Nanobody
NF-κB	Nuclear factor-kappaB
NGF	Nerve growth factor
NMR	Nuclear magnetic resonance
NNGH	N-Isobutyl-N-(4-methoxyphenylsulfonyl)glycyl hydroxamic acid
SAMs	Self-assembled monolayers
SDF	Silver diamine fluoride
SDS-PAGE	Sodium dodecyl sulfate - polyacrylamide gel electrophoresis
STS	Static tensil strain
TB	Tuberculosis
TGF	Transforming growth factor
Th	Helper T cells
TIMP	Tissue inhibitor of matrix metalloproteinase
TNF	Tumor necrosis factor
Trx	Thioredoxin

CHAPTER 1.
BIOLOGICAL MECHANISMS OF ACTION OF MMP-8 IN INFLAMMATORY DISEASE STATES AND THE CHEMICAL MECHANISMS OF ITS INHIBITORS FOR CONTROLLING DISEASE PROCESSES

1.1 INTRODUCTION

Matrix metalloproteinase (MMP)-8 is a member of the MMP family of enzymes that catalyze hydrolysis of proteinaceous substrates. The large MMP family consists of 25 vertebrate MMPs, 23 of which are present in humans [1, 2]. MMPs are Zn^{2+}-dependent proteinases that can be separated into collagenases, gelatinases, stromelysins, matrilysins, and membrane-type MMPs. MMP-8 falls into the collagenase group and is also referred to as collagenase-2 or neutrophil collagenase [1]. As other names imply, MMP-8 is involved in the cleavage of collagen and was thought originally to be expressed solely by neutrophils. However, further studies have identified MMP-8 expression in several other cell types, including odontoblasts, epithelial cells, and macrophages [3, 4]. With expression by many cell types, MMP-8 plays a role in several inflammatory diseases, such as periodontitis, sepsis, asthma and rheumatoid arthritis, and cancers [5, 6], and as such is a sought after target of drug design.

1.2 BIOLOGICAL ROLE OF MMP-8

MMP-8 plays a role in the breakdown of extracellular matrix for tissue remodeling and repairs by cleaving collagen fibers. MMP-8 cleaves type I collagen fibers more efficiently than type II and III collagen fibers and cleaves the fibers at a specific site three-fourths from the N-terminus, resulting in a three-fourth length N-terminal peptide and a one-fourth length C-terminal peptide [5, 7-10]. Overexpression of MMP-8 can lead to increased breakdown of collagen and exacerbation of inflammatory response. MMP-8 is also involved in cancer progression and has long been thought to promote the growth of cancerous tumors, but more recent findings have demonstrated that the presence of MMP-8 in the initial stages of cancer can

limit tumor formation and spreading [5, 6]. In studying the importance of MMP-8 in diseases, several clinical studies have focused on the elevated expression of MMP-8 in the presence of periodontal diseases. MMP-8 expression levels in gingival crevicular fluid (GCF), saliva, and serum have been positively correlated with the presence of periodontitis, periodontal disease severity, and several periodontal clinical parameters [11-14]. When patients undergo nonsurgical periodontal treatment, MMP-8 levels decrease toward a non-disease level concomitant with a decrease in the severity of the periodontitis [14-18]. Because MMP-8 levels are closely and positively correlated with the presence of periodontitis, several enzyme-linked immunosorbent assay (ELISA) and immunofluorometric assay (IFMA) chair-side tests have been developed for easier, cheaper, and noninvasive diagnosis by clinicians using GCF [19-22].

Altered MMP-8 levels have been observed in other inflammatory diseases, including rheumatoid arthritis [23], asthma [24], chronic obstructive pulmonary disease (COPD) [25, 26], and sepsis [27, 28]. Often, increased MMP-8 levels are associated with worsened disease severity. However, in some cancers, MMP-8 serves a protective, anti-tumor role. For example, MMP-8 deficient mice (heterozygous and null) had a faster onset of mammary gland tumors and metastasis in the lungs compared to wild-type mice [29]. Previous review articles have further explained the presence of MMP-8 in inflammatory diseases and cancer and provided more information about the clinical relevance of MMP-8 [5, 6, 30-34]. Although much of the literature involving MMP-8 is based on clinical studies, the purpose of this chapter is to summarize the mechanistic action of MMP-8 that underlies its role in these diseases.

1.3 MECHANISTIC/FUNCTIONAL ROLE IN INFLAMMATION

Because the involvement of MMP-8 in inflammatory diseases and cancers is complex, functional studies of the enzyme have been important for providing insights to explain the

mechanistic roles of MMP-8 in these disease processes. MMP-8 has a complex role in disease progression through involvement in the regulation of inflammatory mediators, macrophage and immune cell migration, and tissue repair and regeneration. During immune response, several inflammatory cytokines are released, mainly from helper T cells (Th) and macrophages, and affect cell-cell interactions and communications [35]. Pro-inflammatory cytokines, such as interleukin (IL)-6, IL-1β, and tumor necrosis factor (TNF)-α, upregulate inflammatory reactions, and anti-inflammatory cytokines, such as IL-4 and IL-10, help to control the pro-inflammatory response. Upregulation of MMP-8 in disease states disrupts the normal balance of cytokines and can lead to worsening of the disease through increased inflammation (Figure 1.1).

1.3.1 Regulation of Inflammatory Mediators

MMP-8 regulates multiple inflammatory mediators in several inflammatory diseases and cancers. In cancer cells with demonstrated increased expression of MMP-8, IL-6 and IL-8 had increased expression compared to control and MMP-8 mutant cells, suggesting that MMP-8 participates in the regulation of these pro-inflammatory mediators during tumor metastasis and tissue repair [36]. Furthermore, studies of MMP-8 null mice resulted in decreased neutrophil infiltration in the lung and decreased circulating levels of IL-6 and IL-1β pro-inflammatory cytokines in sepsis mice models [27]. MMP-8 has been found to activate lipopolysaccharide-induced CXC chemokine (LIX) chemotactic activity by cleaving the precursor LIX, and activated LIX modulates and increases neutrophil infiltration [37]. Some cytokines, such as IL-1β, are produced as precursor proteins, and other MMPs have been found to activate cytokines by proteolytic removal of the N-terminal part [38]. MMP-8 likely functions in a similar manner as other MMPs to regulate cytokine activity. Cytokine regulation can also result from further

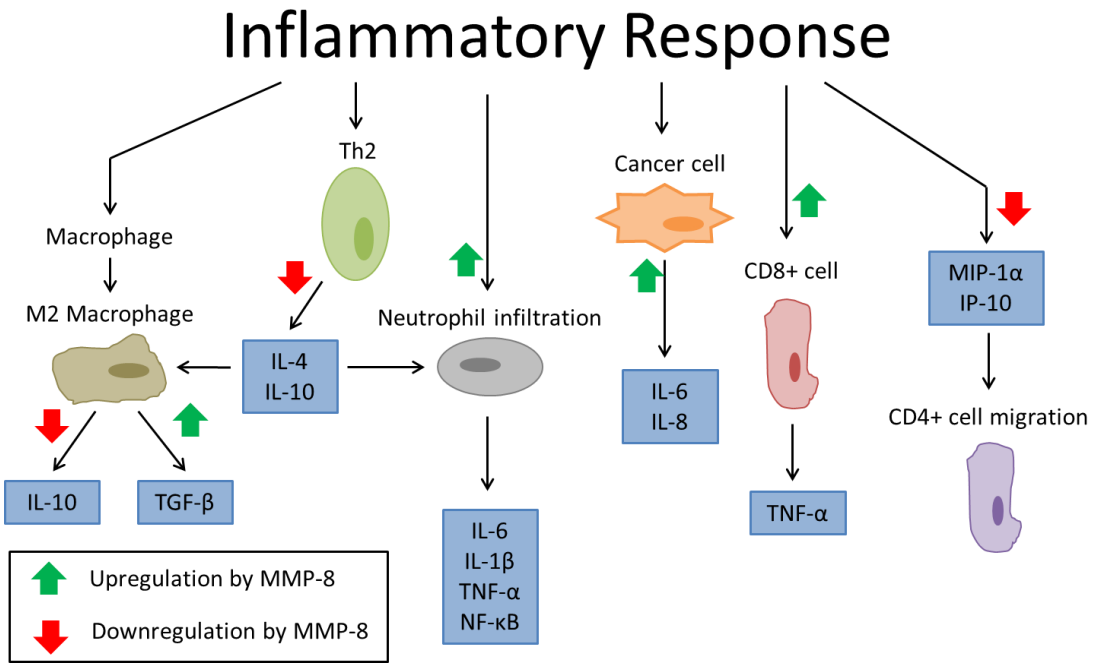

Figure 1.1 Regulatory role of MMP-8 in inflammatory response. MMP-8 upregulates and downregulates several cytokines and influences several processes, including macrophage differentiation, neutrophil infiltration, and lymphocyte migration. MMP-8 expression levels cause changes the levels cytokines and the process during inflammatory response.

cleavage, in a manner similar to collagen cleavage, and inactivation of mature cytokines. MMP-8 regulation of pro-inflammatory mediators is important for disease severity and progression.

MMP-8 also contributed to increased inflammation in ventilator-induced lung injury. Genetic and pharmacological elimination of MMP-8 results in reduced inflammation and increased levels of anti-inflammatory cytokines (IL-4, IL-10) in lung tissue and fluid in mice after high-pressure ventilation compared to wild-type mice [39]. MMP-8 may play a role in neutrophil apoptosis by controlling neutrophilic and eosinophilic recruitment into allergen-induced lung inflammation [40]. Additionally, IL-4 activates rearrangement of neutrophil cytoskeleton, potentially activates neutrophilic protein synthesis, and delays neutrophil apoptosis

[41]. Upregulation of IL-4 in the absence of MMP-8 suggests that IL-4 also modulates neutrophil recruitment. It is possible that MMP-8 may not directly control neutrophil apoptosis and inflammation and may be controlling indirectly these processes by regulating IL-4 cytokine levels. As for IL-10, MMP-8 regulates IL-10 by cleaving and thus inactivating the cytokine [42]. In the absence of MMP-8 enzymatic action, IL-10 levels increase, and inflammation decreases.

In neuroinflammatory disorders, such as sepsis, MMP-8 is involved in inflammatory regulation of TNF-α, a pro-inflammatory cytokine [43]. It is also possible that MMP-8 activates the pro-inflammatory transcription factor-nuclear factor-kappaB (NF-κB) and causes increased inflammation [27]. The role of MMP-8 as a regulator of several inflammatory mediators makes MMP-8 a key target for treatment of many inflammatory diseases. Targeting MMP-8 with inhibitors will shut down MMP-8 enzymatic function and result in decreased inflammation and improved disease prognosis. Because this enzyme can exert different effects on unique disease states at individual stages of disease progression, understanding the complex behavior and involvement of MMP-8 is critical for achieving the desired therapeutic effect.

1.3.2 Immune Cell and Macrophage Migration

MMP-8 indirectly causes reduced migration of macrophages and CD4+ lymphocytes into lungs after lung injury. Upregulation of MMP-8 causes decreased macrophage inflammatory protein (MIP)-1α and interferon-γ inducible protein (IP)-10 lung levels, which reduced migration of macrophages and CD4+ lymphocytes [44]. MMP-8 restrains lung inflammation by cleaving and inactivating MIP-1α [45]. Reduced levels of IP-10 can be explained by fewer macrophages activated by MIP-1α because a significant source of IP-10 is from activated macrophages [46]. Reduced migration of macrophages and CD4+ lymphocytes is expected because MIP-1α is a

potent chemoattractant for macrophages [47] and lymphocytes [48], which are increased by IP-10 in lung inflammation models [49].

Contradictory results regarding MMP-8 and CD8+ T cells were reported in a separate study involving children with gingivitis and Down syndrome. In this study, a significant positive correlation between MMP-8 and CD8+ T cells was observed [50]. Individuals with Down syndrome have altered immune responses due to reduced chemotactic ability, interruptions in T- and B-cell subpopulations, and impaired polymorphonuclear leukocytes phagocytosis [51-53]. In children with Down syndrome and altered immune response, it is possible that MMP-8 facilitates migration of immune cells into periodontal tissue, which does not occur in controls, and this may lead to more extensive periodontal tissue degradation [50].

MMP-8 also controls transforming growth factor (TGF)-β bioactivity, which indicates a role of MMP-8 involvement in macrophage differentiation and polarization through promoting M2-macrophage differentiation [54]. MMP-8 deficient macrophage culture media had a lower level of TGF-β compared to wild-type macrophage culture media. It has been demonstrated that TGF-β levels in lung, especially macrophages, is decreased by IL-10 [55]. Because MMP-8 cleaves IL-10, it is possible that the enzyme indirectly prevents inhibition of TGF-β by decreasing IL-10 levels.

1.3.3 Tissue Repair and Regeneration

MMP-8 is a key component of dentin collagen degradation. In an *in vitro* study, dentin collagen fibrils changed and disappeared several hours after treatment with MMP-8. However, the degradation was prevented when the collagen fibrils were treated with chlorhexidine or captopril in the solution to inhibit MMP-8 [56]. MMP-8 was detected in the mineralized and non-mineralized compartments of human dentin. No other MMPs were detected which suggests

that MMP-8 is the major collagenase in dentin. The lesser amounts of MMP-8 compared to dental gelatinases bound to mineralized dentin suggest that MMP-8 may be more involved in dentin matrix organization than mineralization [57].

In a study with MMP-8 null mice, it was found that MMP-8 is involved in tongue wound healing by regulating TGF-β1 (Figure 1.2). MMP-8 null mice and MMP-8 null fibroblasts had higher expression levels of TGF-β1 than wild-type mice and fibroblasts [58]. MMP-8 was found to inhibit TGF-β1 activity through the cleavage of decorin in a breast cancer cell study [59]. In MMP-8 null mice, tongue wounds healed faster initially (6-24 hours) compared to wild-type mice, which suggests that MMP-8 delays the wound healing process [58]. The opposite effect was seen for skin wounds which healed faster in wild-type mice than MMP-8 null mice [60]. In the latter study, MMP-8 null mice also exhibited lower levels of active TGF-β1 and increased levels of pSmad2 and pSmad3, TGF-β1 intracellular effectors. TGF-β1 signaling regulates wound healing processes [61, 62], and these results suggest that TGF-β1 and members of the Smad family contribute to the increased neutrophil infiltration observed in MMP-8 null mice [60]. MMP-8 null mice also had

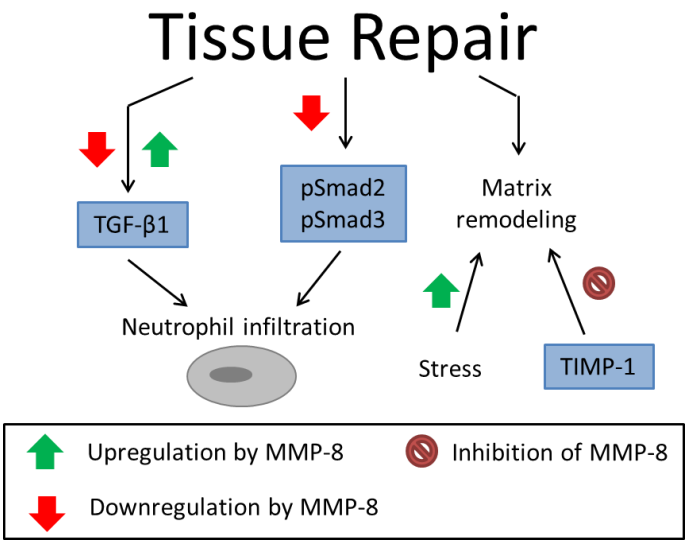

Figure 1.2 Role of MMP-8 in tissue repair. MMP-8 has been found to both upregulate and down regulate TGF-β1 and downregulates TGF-β1 intracellular effectors, pSmad2 and pSmad3, during tissue repair and regeneration. MMP-8 is upregulated under high stress conditions while TIMP-1 regulates matrix remodeling by inhibiting MMP-8. The balance of MMP-8 upregulation and inhibition is important for healthy wound healing.

decreased neutrophil apoptosis, which possibly leads to continued inflammation in skin wounds [60]. TGF-β1 activation by MMPs has also been demonstrated in several other studies [63-65]. MMP-8 regulation of TGF-β1 plays an important role in healing and inflammation.

Stress and strain cause differences in expression of MMP-8 and affect inflammation and healing. In addition to delayed healing of chronic wounds [66, 67], overexpression of MMP-8 may be linked to stress-impaired healing of acute wounds with persisting high levels of neutrophils at the wound site. When wounds of stressed and non-stressed mice were compared, differences in orientation of collagen fibrils were observed. These differences potentially associate MMP-8 overexpression with poorer collagen formation in wound healing, which results in scarring [68]. The disorganization and poor architecture of collagen fibrils in stressed mice caused greater scarring at the wound sites. A study using human periodontal ligament fibroblasts (HPdLF) found that high static tensile strain (STS) of 10% was needed to cause significantly increased production of MMP-8, an indicator of periodontal inflammation and extracellular degradation. However, tissue inhibitor of matrix metalloproteainase (TIMP)-1 levels were also elevated at 10% STS, so high STS most likely causes extracellular matrix alteration, rather than degradation, since TIMP-1 binds to and inhibits MMP-8 (Figure 1.2) [69]. Through inhibition, TIMP-1 controls MMP-8 activity and prevents complete degradation of the extracellular matrix.

MMP-8 is also associated with the immune response related to cellular death through tissue necrosis, a negative, pro-inflammatory outcome of wound healing. During necrosis, the plasma membrane rapidly becomes permeable and cellular contents are released to the intracellular space, often inducing an inflammatory response [70]. The presence of MMP-8 at the necrotic site may aid in the recruitment of neutrophils for immune response [71]. Increased

levels of MMP-8 at a site of necrosis also are important for collagen breakdown in tissue remodeling during necrosis. In tissue remodeling, MMP-8 expression is present in nerve fibers, including nerve fiber growth cones and is upregulated by the nerve growth factor (NGF) in cultured neurons. MMP-8 plays an important role in nerve fiber penetration into collagen I fibers. When MMP-8 was inhibited or neutralized by an antibody, nerve fibers did not penetrate and extend into the basement membrane, and nerve fiber growth was blocked by collagen fibers. It is possible that nerve fibers release MMP-8, which cleaves the nearby collagen fibers, to stimulate nerve growth into the collagen matrix [72].

1.4 INHIBITION

Overexpression of MMP-8 in inflammatory diseases and some cancers causes deleterious effects, as seen with the roles of MMP-8 described above. MMP-8 is a useful biomarker and serves as a good drug target in the treatment of these diseases. The presence of MMP-8 during disease progression leads to increased inflammation and worsening of disease state, and inhibiting the enzyme would allow for faster, improved recovery. MMP-8 levels are consistently elevated in inflammatory diseases, whereas the expression levels of other biomarkers have been found to vary. MMP-8 also regulates several inflammation and tissue repair pathways that affect disease outcome, making MMP-8 a good drug target. MMP-8 and similar enzymes serve important regulatory functions throughout the body, so complete inhibition of MMP-8 would prevent necessary functions and lead to even greater health problems. Inhibition of MMP-8 can be accomplished in a number of ways, but achieving potent, selective inhibition at the site of aberrant activity has proven very challenging because of the ubiquitous expression and need for MMP-8 and related enzymes in normal, healthy tissue function throughout the body [73, 74].

Various approaches have been investigated for the development of MMP-8 inhibitors. Both small and large molecules have proven to be effective at blocking MMP-8 activity. In the development of inhibitors, the enzyme's catalytic site is the main target to block the active site and prevent cleavage of collagen fibers. Other inhibitors bind to sites nearby the MMP-8 catalytic site and sterically block collagen from entering the active site. Inhibition of MMP-8 also obstructs the enzyme's regulatory role in inflammatory response and tissue repair.

The structure of MMP-8 is important for understanding the mechanisms of inhibitor interaction. A crystal structure revealed a smaller α-helical C-terminal subdomain separated from a larger N-terminal domain, composed of two α-helices, a five-stranded β-sheet, and bridging loops, by an active-site cleft [75]. The catalytic domain holds a catalytic Zn^{2+} ion at the bottom of the cleft and another non-exchangeable Zn^{2+} ion and two Ca^{2+} ions on top of the β-sheet (Figure 1.3). When collagen fibers, each comprised of two α1-chains and one α2-chain, undergo cleavage, the α2-chain unwinds from the rest of the fibril, orients into the active-site cleft, and interacts with the catalytic Zn^{2+} ion and nearby MMP-8 residues (Figure 1.4) [76]. In addition to the active site, MMP-8 has additional active sites known as subsites (S), which can interact with substrates [77, 78]. Subsites S*n* and S*n*' are on the left and the right of the catalytic Zn^{2+} ion, respectively, and some of the subsites are labeled in Figure 1.5A. The sites on the substrates or inhibitors that interact with the subsites are termed P*n* and P*n*', respectively. The S1' pocket is the substrate binding site next to the catalytic Zn^{2+} ion and is a main contributor to determination of inhibitor affinity [79]. Developing inhibitors that interact with MMP-8 in a similar manner as α2-chain would prevent the collagen fibrils from entering the active-site cleft and being cleaved.

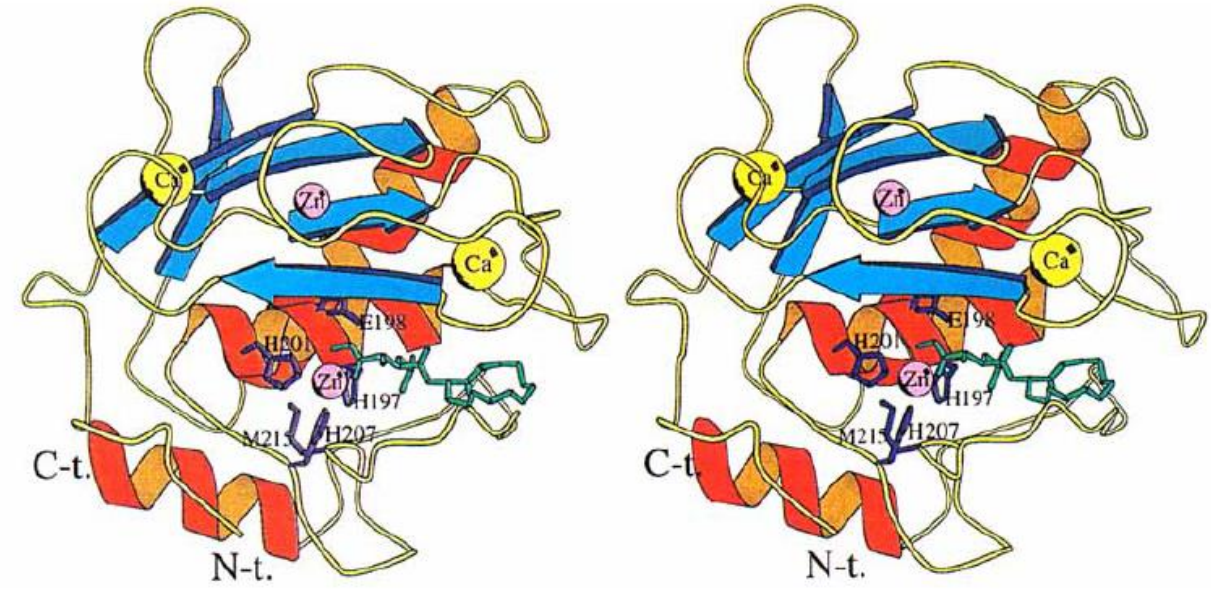

Figure 1.3 Stereo plot ribbon model of MMP-8 (79-242) from crystal structure. A five-stranded β-sheet and two α-helices make up the N-terminal domain of MMP-8, and the C-terminal domain consists of one α-helix. The catalytic Zn^{2+} ion is held in the active site by three histidine residues (purple sticks), and the other Zn^{2+} and two Ca^{2+} ions are positioned above the β-sheet. Bound BB-1909 inhibitor is shown as a green stick model interacting with the catalytic Zn^{2+} ion. Reproduced with permission from *Eur. J. Biochem*. 247, 356-363 © 1997 FEBS [75].

Effective inhibitors would interact with the catalytic Zn^{2+} ion and hydrogen bond to residues in the active site to prevent MMP-8 interaction with collagen.

Inhibition of MMP-8 has been demonstrated with the use of silver diamine fluoride (SDF) [80]. Increasing percentages of SDF showed greater inhibition. The investigators also tested NaF and $AgNO_3$ at equivalent amounts of fluoride and silver, respectively. The percentage of MMP-8 inhibition was significantly higher by the SDF solutions than the NaF and $AgNO_3$ solutions, but the mechanism of inhibition is unknown. In clinical studies, the use of SDF has shown potential to prevent progression of dental caries [81-83]. In spite of the potential anti-caries benefits, SDF has not realized widespread adoption because the treated teeth are stained black. Inhibition of MMP-8 with SDF prevents enzymatic degradation of dentin.

Sepsis model rats had elevated MMP-8 expression levels in the myocardium compared to control rats. Sepsis model rats that underwent treatment with dexamethasone (DEX) had statistically identical MMP-8 levels compared with untreated sepsis rats [84]. DEX treatment has been shown to reduce expression levels of other MMPs [85, 86] but did not have the same effect on MMP-8. However, significantly lower MMP-8 expression was observed in sepsis rats after treatment with the MMP-8 inhibitor M8I ((3R)-(+)-[2-(4-Methoxybenzenesulfonyl)-1,2,3,4-tetrahydroisoquinoline-3-hydroxamate]). M8I may improve the outcome of sepsis induced myocardial injury [84]. Inhibition of MMP-8 in sepsis patients reduces the levels of pro-inflammatory cytokines IL-1β and TNF-α which may lessen the degree of myocardial injury.

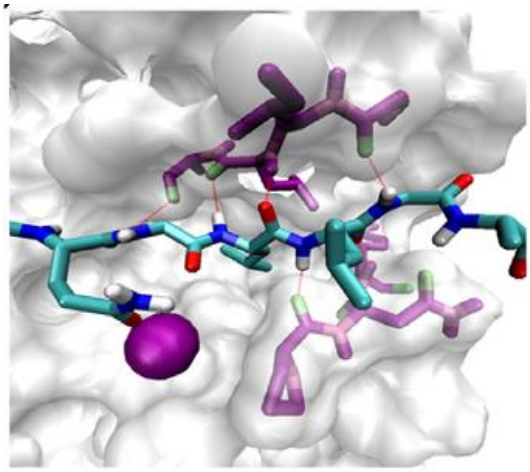

Figure 1.4 MMP-8 cleavage of collagen. The collagen α2 chain, in the MMP-8 active site, interacts with the catalytic Zn^{2+} ion (purple sphere) and H-bonded to MMP-8 residues (red lines). Modified and reproduced with permission from *J. Mol. Biol.* 425, 1815–1825 © 2013 Elsevier [76].

In the case of tuberculosis (TB), NF-κB inhibitors p65 subunit helenalin, caffeic acid phenethyl ester (CAPE), and SN50 inhibited MMP-8 production while maintaining neutrophil activity. These NF-κB inhibitors prevented neutrophil secretion of MMP-8 and may prevent tissue destruction by MMP-8 in patients with TB. Collagen destruction was also decreased by a MMP-8 neutralizing antibody. Neutrophil collagenase activity was reduced to normal in TB patients treated with doxycycline [87]. Inhibition of MMP-8 by doxycycline is in line with previous studies [88, 89]. Doxycycline inhibition is not specific for MMP-8 and interacts with domains of other MMPs. A study with truncated enzymes suggests that doxycycline disrupts the conformation of the catalytic domain of MMP-8 [90].

MMP-8 activity was also inhibited in human neutrophils when incubated with chlorohexidine (CHX) [91]. Addition of calcium chloride prevented MMP-2 and MMP-9 inhibition by CHX, which suggests that CHX may inhibit the MMPs through a chelating mechanism. Inhibition through cation chelation was also suggested in a study of MMP-8 inhibition by dichloromethylene bisphosphonate (clodronate) [92]. *In vivo*, chelation of the catalytic Zn^{2+} ion or structural Zn^{2+} and Ca^{2+} ions in MMP-8 is not a selective approach for inhibition. Many enzymes and other proteins depend on binding to metal ions for their function and/or structure and are disrupted by treatment with chelators [93]. The unintended removal of metal ions from other enzymes by chelators leads to more diverse side effects, so caution must be taken when inhibiting MMP-8 through chelation.

Inhibitor interaction with the MMP-8 catalytic Zn^{2+} ion has previously been studied [94]. The crystal structure of MMP-8 with BB-1909, a derivative of the broad-spectrum MMP inhibitor batimastat, display the catalytic Zn^{2+} liganded by the three histidine nitrogen atoms in MMP-8 and by the hydroxyl oxygen and carbonyl oxygen of the hydroxamate group of BB-1909 in a bidentate manner (Figure 1.3). The side chain of Glu198 also coordinates with the hydroxamate hydroxyl, and the carbonyl of Ala161 and Glu198 coordinate with the hydroxamate nitrogen. Further, the orientation of the isobutyl group extends into the S1’ pocket of MMP-8. With similar molecular structure, BB-1909 and batimastat have almost equivalent interaction with MMP-8. The barbiturate ring of a barbiturate acid derivative (RO200-1770) interacts with MMP-8 in similar structural orientation as batimastat (Figure 1.5) [95]. Both the barbiturate ring of RO200-1770 and batimastat orient into the S1’ and S2’ pockets of MMP-8 while the N3 and O2 of the barbiturate ring and N and O of batimastat coordinate the Zn^{2+} ion.

MMP-8 inhibition is also possible through inhibitor interaction outside of the active site, such as with antibodies and derivatives of these large molecules. A nanobody (Nb), which is derived from a *Camelidae* heavy-chain-only antibody, showed micromolar inhibition of mouse (mMMP-8) and human MMP-8 but very limited binding to other MMPs and metalloproteinases [96]. The Nbs were produced by immunization of *Alpacas* with the catalytic domain of mMMP-8, and they did not interact with several other MMPs. Macromolecular inhibitors are a growing class of therapeutics because of their exceptional selectivity, specificity, high affinity, longer circulation time, and minimal toxicity. They are a very good option for extracellular targets like

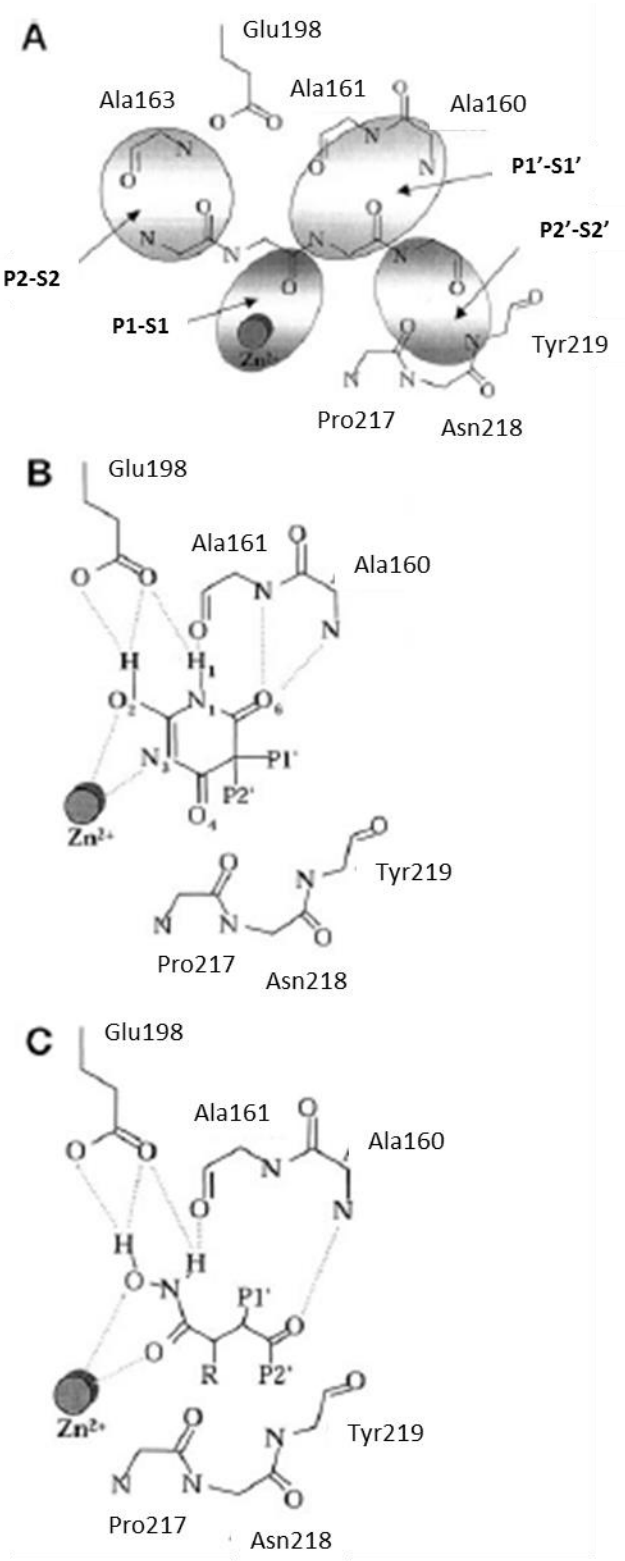

Figure 1.5 MMP-8 substrate recognition site. (A) Representation of the interaction between MMP-8 and its substrates. The subsites, S*n* and S*n*', and the interaction sites on the substrate, P*n* and P*n*', are labeled. (B) Interaction of RO200-1770, a barbiturate acid derivative, with the MMP-8 active site. (C) Representation of batimastat interaction with the MMP-8 active site. Reproduced with permission from *J. Biol. Chem*. 276, 17405–17412 © 2001 The American Society for Biochemistry and Molecular Biology, Inc. [95].

MMPs. Nb are smaller than antibodies and are retained in circulation for a shorter length of time. This molecule demonstrates selective inhibition of MMP-8 by a Nb, but the affinity and circulating half-life need to be improved to generate a clinically relevant lead candidate. Because larger molecules are retained in circulation longer, conjugation to increase the size of small proteins has been used to extend their time in the bloodstream [97-101]. When the Nb was conjugated with an anti-albumin Nb, a significantly longer half-life was achieved (28 hrs compared to 2 hrs without the anti-albumin Nb) and the conjugate maintained equivalent MMP-8 binding and inhibitory abilities [96]. The specific interaction between this Nb and MMP-8 has not been determined experimentally, but computer modeling suggests that the Nb most likely binds to one of three possible locations, one at the active site and two outside the active site but still on the catalytic domain (Figure 1.6). The active site and another location might involve lysine residue recognition. Further testing revealed that the Nb most likely binds to one of the

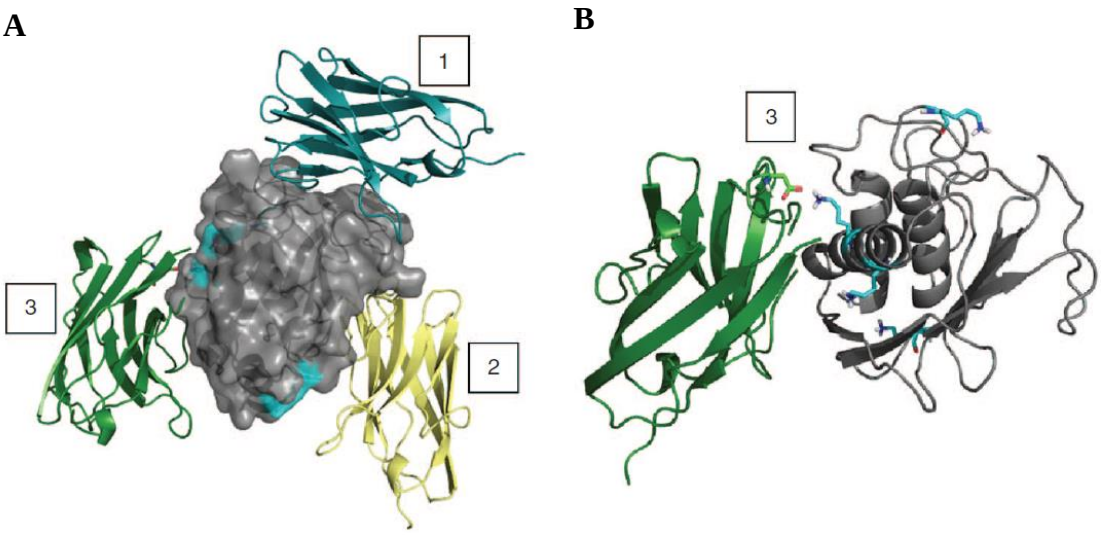

Figure 1.6 Nanobody (Nb) inhibitor interactions with MMP-8. (A) MMP-8 catalytic domain in gray has lysine residues on the surface, shown in cyan. The three locations indicate predicted Nb inhibitor binding places, shown by the Nb conformations in cyan (1), yellow (2), and green (3). The interaction with Nb in (2) occurs at the MMP-8 active site. (B) Stick conformation of lysine-lysine interaction between MMP-8 (gray) and Nb (green) is shown. Reproduced with permission from *Mol. Ther.* 24, 890-902 © 2016 The American Society for Biochemistry and Molecular Biology, Inc. [96].

locations outside the active site and causes inhibition through steric hindrance or conformational changes of MMP-8. This initial success suggests that with modification to improve binding affinity this approach may be useful in the clinic.

In addition to direct inhibitor interaction with MMP-8, other approaches have been investigated to inhibit the effects of MMP-8 action on its matrix substrates, including dentin. Dentin is composed of a collagenous matrix that largely is mineralized with hydroxylapatite but also contains substantial amounts of water and organic material [102]. The organic material is made up of 90% collagen, almost all type I, and 10% non-collagenous proteins and proteoglycans. Mineralization of dentin, through crystallization of calcium phosphate, hardens the tooth tissue, which is important for physiological function [102]. MMP-8 enzymatic action results in the cleavage of collagen fibers and ultimately the breakdown of dentin, which supports caries formation [103, 104]. Treatment of dentin with collagen crosslinkers, such as grape seed extracts, sumac extracts, and riboflavin, resulted in decreased levels of extractable dentinal MMP-8 compared to controls, as determined by zymography and enzyme activity assays [105]. Treatment with these compounds most likely covalently crosslinks collagen fibers, decreasing the size exclusion cut-off of the collagen matrix and preventing MMP-8 from being released. The crosslinking of collagen makes it more difficult to unwind the fibers, which slows cleavage of the collagen chains. Crosslinker treatment also results in covalent attachment of the enzyme to the matrix and inactivation of MMP-8. Although this approach is less likely to be used in therapeutic applications, it may have relevance to implanted biological restorations to inhibit the destructive action of MMP-8 *in situ* and increase longevity of the restoration.

Although the inhibitors discussed above decrease expression of or inhibit MMP-8 by binding to it, the exact mechanism by which inhibition is accomplished has not yet been

delineated for several MMP-8 inhibitors. Determination of the exact mechanism of a compounds' inhibition is critical for achieving the desired effect for enzymes with broad expression in the body. Recent studies have suggested a possible mechanism of MMP-8 inhibition by the tether-MAP peptide [106-108]. The metal abstraction peptide (MAP) is composed of the amino acid sequence NCC, and under neutral to basic pH it scavenges metal ions from other molecules [109]. Initial studies demonstrated that when chemically conjugated to 2-aminoethyl methacrylate hydrochloride (AEMA) containing dental polymers, tether-MAP binds MMP-8 and inhibits enzymatic action. Based on understanding of the MAP peptide chemistry, it was hypothesized that inhibition is accomplished via the Zn^{2+} ion in MMP-8's catalytic active site [106]. Additional investigation using self-assembled monolayers (SAMs) further support that the MAP Tag directly interacts with and confirms that it inhibits MMP-8 through the Zn^{2+} ion in the active site [107].

Follow up studies, similar to the surface studies on the dental polymers and SAMs, are needed to gain a better understanding of the intermolecular interaction between MMP-8 and MAP and to elucidate the specific mechanism of inhibition. This approach is advantageous because MAP has exceptionally high affinity and reduced toxicity compared to other small molecule inhibitors of MMP-8 and acts as a very slowly reversible inhibitor to mitigate the destructive activity of this enzyme *in situ*. Tether-MAP provided proof of concept, demonstrating the viability of using this peptide module to inhibit MMP-8, but this construct was not optimized to achieve selectivity solely for MMP-8. Because it is a peptide, the sequence around the metal-binding module may be modified using standard screening techniques and/or rational design approaches to generate a molecule that more specifically interacts with MMP-8 to accomplish selective inhibition.

1.5 CONCLUSIONS

Although MMP-8 is used as a biomarker for several diseases, it also contributes to disease severity and outcome. This insight into the mechanistic role of MMP-8 in inflammatory diseases and cancer has linked together events of MMP-8 regulation of inflammatory mediators and proteins involved in tissue repair, neutrophil migration, and inflammation. To improve patient outcomes of relevant disease states, several approaches are available for inhibition of MMP-8. Further studies are needed to investigate the mechanism of inhibitor interaction with MMP-8 to continue to develop more specific inhibitors, but understanding the multiple regulation events of MMP-8 is useful for understanding how MMP-8 participates in disease progression.

1.6 REFERENCES

1. Visse, R. and H. Nagase, *Matrix metalloproteinases and tissue inhibitors of metalloproteinases: Structure, function, and biochemistry.* Circulation Research, 2003. **92**(8): p. 827-839.
2. Parks, W.C., C.L. Wilson, and Y.S. Lopez-Boado, *Matrix metalloproteinases as modulators of inflammation and innate immunity.* Nat Rev Immunol, 2004. **4**(8): p. 617-629.
3. Palosaari, H., J. Wahlgren, M. Larmas, H. Rönkä, T. Sorsa, T. Salo, and L. Tjäderhane, *The expression of MMP-8 in human odontoblasts and dental pulp cells is down-regulated by TGF-β1.* Journal of Dental Research, 2000. **79**(1): p. 77-84.
4. Prikk, K., E. Pirilä, R. Sepper, P. Maisi, T. Salo, J. Wahlgren, and T. Sorsa, *In vivo collagenase-2 (MMP-8) expression by human bronchial epithelial cells and monocytes/macrophages in bronchiectasis.* The Journal of Pathology, 2001. **194**(2): p. 232-238.
5. Van Lint, P. and C. Libert, *Matrix metalloproteinase-8: Cleavage can be decisive.* Cytokine & Growth Factor Reviews, 2006. **17**(4): p. 217-223.
6. Dejonckheere, E., R.E. Vandenbroucke, and C. Libert, *Matrix metalloproteinase-8 has a central role in inflammatory disorders and cancer progression.* Cytokine & Growth Factor Reviews, 2011. **22**(2): p. 73-81.
7. Lu, P., K. Takai, V.M. Weaver, and Z. Werb, *Extracellular matrix degradation and remodeling in development and disease.* Cold Spring Harbor perspectives in biology, 2011. **3**(12): p. 10.1101/cshperspect.a005058 a005058.
8. Nagase, H., R. Visse, and G. Murphy, *Structure and function of matrix metalloproteinases and TIMPs.* Cardiovascular Research, 2006. **69**(3): p. 562-573.
9. Visse, R. and H. Nagase, *Matrix metalloproteinases and tissue inhibitors of metalloproteinases: structure, function, and biochemistry.* Circ Res, 2003. **92**(8): p. 827-39.
10. Fields, G.B., *Interstitial collagen catabolism.* Journal of Biological Chemistry, 2013. **288**(13): p. 8785-8793.

11. Kraft-Neumärker, M., K. Lorenz, R. Koch, T. Hoffmann, P. Mäntylä, T. Sorsa, and L. Netuschil, *Full-mouth profile of active MMP-8 in periodontitis patients.* Journal of Periodontal Research, 2012. **47**(1): p. 121-128.
12. Gupta, N., N.D. Gupta, A. Gupta, S. Khan, and N. Bansal, *Role of salivary matrix metalloproteinase-8 (MMP-8) in chronic periodontitis diagnosis.* Frontiers of Medicine, 2014. **9**(1): p. 72-76.
13. Nizam, N., P. Gümüş, J. Pitkänen, T. Tervahartiala, T. Sorsa, and N. Buduneli, *Serum and salivary matrix metalloproteinases, neutrophil elastase, myeloperoxidase in patients with chronic or aggressive periodontitis.* Inflammation, 2014. **37**(5): p. 1771-1778.
14. Anovazzi, G., M.C.d. Mendeiros, T.M. Ferrisse, S.C.T. Corbi, L.S. Finota, M.H. Tanaka, A.M. Marcaccini, S.R.P. Orrico, J.A. Cirelli, R.F. Gerlach, and R.M.S. Caminaga, *Haplotypes of susceptibility to chronic periodontitis do not influence MMP-8 levels or the outcome of non-surgical periodontal therapy.* Journal of Dentistry and Research, 2014. **1**(1): p. 4-14.
15. Romero, A.M., P. Mastromatteo-Alberga, L. Escalona, and M. Correnti, *[MMP-3 and MMP-8 levels in patients with chronic periodontitis before and after nonsurgical periodontal therapy]*. Invest Clin, 2013. **54**(2): p. 138-48.
16. Meschiari, C.A., A.M. Marcaccini, B.C. Santos Moura, L.R. Zuardi, J.E. Tanus-Santos, and R.F. Gerlach, *Salivary MMPs, TIMPs, and MPO levels in periodontal disease patients and controls.* Clinica Chimica Acta, 2013. **421**: p. 140-146.
17. Kurgan, Ş., Ö. Fentoğlu, C. Önder, M. Serdar, F. Eser, D.N. Tatakis, and M. Günhan, *The effects of periodontal therapy on gingival crevicular fluid matrix metalloproteinase-8, interleukin-6 and prostaglandin E2 levels in patients with rheumatoid arthritis.* Journal of Periodontal Research, 2015: p. n/a-n/a.
18. Konopka, L., A. Pietrzak, and E. Brzezinska-Blaszczyk, *Effect of scaling and root planing on interleukin-1beta, interleukin-8 and MMP-8 levels in gingival crevicular fluid from chronic periodontitis patients.* J Periodontal Res, 2012. **47**(6): p. 681-8.
19. Izadi Borujeni, S., M. Mayer, and P. Eickholz, *Activated matrix metalloproteinase-8 in saliva as diagnostic test for periodontal disease? A case-control study.* Med Microbiol Immunol, 2015. **204**(6): p. 665-72.

20. Nieminen, M.T., P. Vesterinen, T. Tervahartiala, I. Kormi, J. Sinisalo, P.J. Pussinen, and T. Sorsa, *Practical implications of novel serum ELISA-assay for matrix metalloproteinase-8 in acute cardiac diagnostics.* Acute Card Care, 2015. **17**(3): p. 46-7.
21. Akbari, G., M.L. Prabhuji, B.V. Karthikeyan, K. Raghunatha, and R. Narayanan, *Analysis of matrix metalloproteinase-8 levels in gingival crevicular fluid and whole mouth fluid among smokers and nonsmokers using enzyme-linked immune-sorbent assay and a novel chair-side test.* J Indian Soc Periodontol, 2015. **19**(5): p. 525-30.
22. Heikkinen, A.M., S.O. Nwhator, N. Rathnayake, P. Mantyla, P. Vatanen, and T. Sorsa, *Pilot study on oral health status as assessed by an active matrix metalloproteinase-8 chairside mouthrinse test in adolescents.* J Periodontol, 2016. **87**(1): p. 36-40.
23. Mattey, D.L., N.B. Nixon, and P.T. Dawes, *Association of circulating levels of MMP-8 with mortality from respiratory disease in patients with rheumatoid arthritis.* Arthritis Res Ther, 2012. **14**(5): p. R204.
24. Obase, Y., P. Rytila, T. Metso, A.S. Pelkonen, T. Tervahartiala, M. Turpeinen, M. Makela, U. Saarialho-Kere, O. Selroos, T. Sorsa, and T. Haahtela, *Effects of inhaled corticosteroids on metalloproteinase-8 and tissue inhibitor of metalloproteinase-1 in the airways of asthmatic children.* Int Arch Allergy Immunol, 2010. **151**(3): p. 247-54.
25. Navratilova, Z., J. Zatloukal, E.V.A. Kriegova, V. Kolek, and M. Petrek, *Simultaneous up-regulation of matrix metalloproteinases 1, 2, 3, 7, 8, 9 and tissue inhibitors of metalloproteinases 1, 4 in serum of patients with chronic obstructive pulmonary disease.* Respirology, 2012. **17**(6): p. 1006-1012.
26. Yildirim, E., I. Kormi, Ö.K. Başoğlu, A. Gürgün, B. Kaval, T. Sorsa, and N. Buduneli, *Periodontal health and serum, saliva matrix metalloproteinases in patients with mild chronic obstructive pulmonary disease.* Journal of Periodontal Research, 2013. **48**(3): p. 269-275.
27. Solan, P.D., K.E. Dunsmore, A.G. Denenberg, K. Odoms, B. Zingarelli, and H.R. Wong, *A novel role for matrix metalloproteinase-8 in sepsis.* Critical Care Medicine, 2012. **40**(2): p. 379-387.
28. Sivula, M., J. Hastbacka, A. Kuitunen, R. Lassila, T. Tervahartiala, T. Sorsa, and V. Pettila, *Systemic matrix metalloproteinase-8 and tissue inhibitor of metalloproteinases-1*

levels in severe sepsis-associated coagulopathy. Acta Anaesthesiol Scand, 2015. **59**(2): p. 176-84.

29. Decock, J., W. Hendrickx, S. Thirkettle, A. Gutierrez-Fernandez, S.D. Robinson, and D.R. Edwards, *Pleiotropic functions of the tumor- and metastasis-suppressing matrix metalloproteinase-8 in mammary cancer in MMTV-PyMT transgenic mice.* Breast Cancer Res, 2015. **17**: p. 38.
30. Sorsa, T., T. Tervahartiala, J. Leppilahti, M. Hernandez, J. Gamonal, A.M. Tuomainen, A. Lauhio, P.J. Pussinen, and P. Mantyla, *Collagenase-2 (MMP-8) as a point-of-care biomarker in periodontitis and cardiovascular diseases. Therapeutic response to non-antimicrobial properties of tetracyclines.* Pharmacol Res, 2011. **63**(2): p. 108-13.
31. Sorsa, T., U.K. Gursoy, S. Nwhator, M. Hernandez, T. Tervahartiala, J. Leppilahti, M. Gursoy, E. Könönen, G. Emingil, P.J. Pussinen, and P. Mäntylä, *Analysis of matrix metalloproteinases, especially MMP-8, in gingival crevicular fluid, mouthrinse and saliva for monitoring periodontal diseases.* Periodontology 2000, 2016. **70**(1): p. 142-163.
32. Mallat, Z., *Matrix metalloproteinase-8 and the regulation of blood pressure, vascular inflammation, and atherosclerotic lesion growth.* Circ Res, 2009. **105**(9): p. 827-9.
33. Lenglet, S., F. Mach, and F. Montecucco, *Role of matrix metalloproteinase-8 in atherosclerosis.* Mediators Inflamm, 2013. **2013**: p. 659282.
34. Ye, S., *Putative targeting of matrix metalloproteinase-8 in atherosclerosis.* Pharmacol Ther, 2015. **147**: p. 111-22.
35. Zhang, J.-M. and J. An, *Cytokines, inflammation and pain.* International anesthesiology clinics, 2007. **45**(2): p. 27-37.
36. Thirkettle, S., J. Decock, H. Arnold, C.J. Pennington, D.M. Jaworski, and D.R. Edwards, *Matrix metalloproteinase 8 (collagenase 2) induces the expression of interleukins 6 and 8 in breast cancer cells.* J Biol Chem, 2013. **288**(23): p. 16282-94.
37. Tester, A.M., J.H. Cox, A.R. Connor, A.E. Starr, R.A. Dean, X.S. Puente, C. Lopez-Otin, and C.M. Overall, *LPS responsiveness and neutrophil chemotaxis in vivo require PMN MMP-8 activity.* PLoS One, 2007. **2**(3): p. e312.

38. Van Lint, P. and C. Libert, *Chemokine and cytokine processing by matrix metalloproteinases and its effect on leukocyte migration and inflammation.* Journal of Leukocyte Biology, 2007. **82**(6): p. 1375-1381.

39. Albaiceta, G.M., A. Gutierrez-Fernandez, E. Garcia-Prieto, X.S. Puente, D. Parra, A. Astudillo, C. Campestre, S. Cabrera, A. Gonzalez-Lopez, A. Fueyo, F. Taboada, and C. Lopez-Otin, *Absence or inhibition of matrix metalloproteinase-8 decreases ventilator-induced lung injury.* Am J Respir Cell Mol Biol, 2010. **43**(5): p. 555-63.

40. Gueders, M.M., M. Balbin, N. Rocks, J.M. Foidart, P. Gosset, R. Louis, S. Shapiro, C. Lopez-Otin, A. Noel, and D.D. Cataldo, *Matrix metalloproteinase-8 deficiency promotes granulocytic allergen-induced airway inflammation.* J Immunol, 2005. **175**(4): p. 2589-97.

41. Girard, D., R. Paquin, and A.D. Beaulieu, *Responsiveness of human neutrophils to interleukin-4: induction of cytoskeletal rearrangements, de novo protein synthesis and delay of apoptosis.* Biochemical Journal, 1997. **325**(Pt 1): p. 147-153.

42. García-Prieto, E., A. González-López, S. Cabrera, A. Astudillo, A. Gutiérrez-Fernández, M. Fanjul-Fernandez, E. Batalla-Solís, X.S. Puente, A. Fueyo, C. López-Otín, and G.M. Albaiceta, *Resistance to bleomycin-induced lung fibrosis in MMP-8 deficient mice is mediated by interleukin-10.* PLoS ONE, 2010. **5**(10): p. e13242.

43. Lee, E.J., J.E. Han, M.S. Woo, J.A. Shin, E.M. Park, J.L. Kang, P.G. Moon, M.C. Baek, W.S. Son, Y.T. Ko, J.W. Choi, and H.S. Kim, *Matrix metalloproteinase-8 plays a pivotal role in neuroinflammation by modulating TNF-alpha activation.* J Immunol, 2014. **193**(5): p. 2384-93.

44. Craig, V.J., P.A. Quintero, S.E. Fyfe, A.S. Patel, M.D. Knolle, L. Kobzik, and C.A. Owen, *Profibrotic activities for matrix metalloproteinase-8 during bleomycin-mediated lung injury.* J Immunol, 2013. **190**(8): p. 4283-96.

45. Quintero, P.A., M.D. Knolle, L.F. Cala, Y. Zhuang, and C.A. Owen, *Matrix Metalloproteinase-8 inactivates macrophage inflammatory protein-1α to reduce acute lung inflammation and injury in mice.* Journal of immunology (Baltimore, Md. : 1950), 2010. **184**(3): p. 1575-1588.

46. Korpi-Steiner, N.L., M.E. Bates, W.M. Lee, D.J. Hall, and P.J. Bertics, *Human rhinovirus induces robust IP-10 release by monocytic cells, which is independent of viral*

replication but linked to type I interferon receptor ligation and STAT1 activation. J Leukoc Biol, 2006. **80**(6): p. 1364-74.

47. Uguccioni, M., M. D'Apuzzo, M. Loetscher, B. Dewald, and M. Baggiolini, *Actions of the chemotactic cytokines MCP-1, MCP-2, MCP-3, RANTES, MIP-1 alpha and MIP-1 beta on human monocytes.* Eur J Immunol, 1995. **25**(1): p. 64-8.
48. Roth, S.J., M.W. Carr, and T.A. Springer, *C-C chemokines, but not the C-X-C chemokines interleukin-8 and interferon-gamma inducible protein-10, stimulate transendothelial chemotaxis of T lymphocytes.* Eur J Immunol, 1995. **25**(12): p. 3482-8.
49. Zeng, X., T.A. Moore, M.W. Newstead, J.C. Deng, N.W. Lukacs, and T.J. Standiford, *IP-10 mediates selective mononuclear cell accumulation and activation in response to intrapulmonary transgenic expression and during adenovirus-induced pulmonary inflammation.* J Interferon Cytokine Res, 2005. **25**(2): p. 103-12.
50. Tsilingaridis, G., T. Yucel-Lindberg, H. Concha Quezada, and T. Modeer, *The relationship between matrix metalloproteinases (MMP-3, -8, -9) in serum and peripheral lymphocytes (CD8+ , CD56+) in Down syndrome children with gingivitis.* J Periodontal Res, 2014. **49**(6): p. 742-50.
51. Barkin, R.M., W.L. Weston, J.R. Humbert, and F. Maire, *Phagocytic function in Down syndrome--I. Chemotaxis.* J Ment Defic Res, 1980. **24 Pt 4**: p. 243-9.
52. Barkin, R.M., W.L. Weston, J.R. Humbert, and K. Sunada, *Phagocytic function in Down syndrome--II. Bactericidal activity and phagocytosis.* J Ment Defic Res, 1980. **24 Pt 4**: p. 251-6.
53. Levin, S., *The immune system and susceptibility to infections in Down's syndrome.* Prog Clin Biol Res, 1987. **246**: p. 143-62.
54. Wen, G., C. Zhang, Q. Chen, A. Luong le, A. Mustafa, S. Ye, and Q. Xiao, *A novel role of matrix metalloproteinase-8 in macrophage differentiation and polarization.* J Biol Chem, 2015. **290**(31): p. 19158-72.
55. Nakagome, K., M. Dohi, K. Okunishi, R. Tanaka, J. Miyazaki, and K. Yamamoto, *In vivo IL-10 gene delivery attenuates bleomycin induced pulmonary fibrosis by inhibiting the production and activation of TGF-beta in the lung.* Thorax, 2006. **61**(10): p. 886-94.
56. Zheng, X., J. Hu, Y. Chen, Y. Zhu, and H. Chen, *AFM study of the effects of collagenase and its inhibitors on dentine collagen fibrils.* J Dent, 2012. **40**(2): p. 163-71.

57. Sulkala, M., T. Tervahartiala, T. Sorsa, M. Larmas, T. Salo, and L. Tjaderhane, *Matrix metalloproteinase-8 (MMP-8) is the major collagenase in human dentin.* Arch Oral Biol, 2007. **52**(2): p. 121-7.

58. Astrom, P., E. Pirila, R. Lithovius, H. Heikkola, J.T. Korpi, M. Hernandez, T. Sorsa, and T. Salo, *Matrix metalloproteinase-8 regulates transforming growth factor-beta1 levels in mouse tongue wounds and fibroblasts in vitro.* Exp Cell Res, 2014. **328**(1): p. 217-27.

59. Soria-Valles, C., A. Gutierrez-Fernandez, M. Guiu, B. Mari, A. Fueyo, R.R. Gomis, and C. Lopez-Otin, *The anti-metastatic activity of collagenase-2 in breast cancer cells is mediated by a signaling pathway involving decorin and miR-21*. Oncogene, 2014. **33**(23): p. 3054-3063.

60. Gutierrez-Fernandez, A., M. Inada, M. Balbin, A. Fueyo, A.S. Pitiot, A. Astudillo, K. Hirose, M. Hirata, S.D. Shapiro, A. Noel, Z. Werb, S.M. Krane, C. Lopez-Otin, and X.S. Puente, *Increased inflammation delays wound healing in mice deficient in collagenase-2 (MMP-8).* Faseb j, 2007. **21**(10): p. 2580-91.

61. Ashcroft, G.S., X. Yang, A.B. Glick, M. Weinstein, J.L. Letterio, D.E. Mizel, M. Anzano, T. Greenwell-Wild, S.M. Wahl, C. Deng, and A.B. Roberts, *Mice lacking Smad3 show accelerated wound healing and an impaired local inflammatory response.* Nat Cell Biol, 1999. **1**(5): p. 260-6.

62. Hosokawa, R., M.M. Urata, Y. Ito, P. Bringas, Jr., and Y. Chai, *Functional significance of Smad2 in regulating basal keratinocyte migration during wound healing.* J Invest Dermatol, 2005. **125**(6): p. 1302-9.

63. Yu, Q. and I. Stamenkovic, *Cell surface-localized matrix metalloproteinase-9 proteolytically activates TGF-beta and promotes tumor invasion and angiogenesis.* Genes Dev, 2000. **14**(2): p. 163-76.

64. Karsdal, M.A., L. Larsen, M.T. Engsig, H. Lou, M. Ferreras, A. Lochter, J.-M. Delaissé, and N.T. Foged, *Matrix metalloproteinase-dependent activation of latent transforming growth factor-β controls the conversion of osteoblasts into osteocytes by blocking osteoblast apoptosis.* Journal of Biological Chemistry, 2002. **277**(46): p. 44061-44067.

65. Mu, D., S. Cambier, L. Fjellbirkeland, J.L. Baron, J.S. Munger, H. Kawakatsu, D. Sheppard, V.C. Broaddus, and S.L. Nishimura, *The integrin αvβ8 mediates epithelial*

homeostasis through MT1-MMP–dependent activation of TGF-β1. The Journal of Cell Biology, 2002. **157**(3): p. 493-507.

66. Nwomeh, B.C., H.X. Liang, I.K. Cohen, and D.R. Yager, *MMP-8 is the predominant collagenase in healing wounds and nonhealing ulcers.* J Surg Res, 1999. **81**(2): p. 189-95.
67. Pirila, E., J.T. Korpi, T. Korkiamaki, T. Jahkola, A. Gutierrez-Fernandez, C. Lopez-Otin, U. Saarialho-Kere, T. Salo, and T. Sorsa, *Collagenase-2 (MMP-8) and matrilysin-2 (MMP-26) expression in human wounds of different etiologies.* Wound Repair Regen, 2007. **15**(1): p. 47-57.
68. Gajendrareddy, P.K., C.G. Engeland, R. Junges, M.P. Horan, I.G. Rojas, and P.T. Marucha, *MMP-8 overexpression and persistence of neutrophils relate to stress-impaired healing and poor collagen architecture in mice.* Brain, behavior, and immunity, 2013. **28**: p. 10.1016/j.bbi.2012.10.016.
69. Jacobs, C., C. Walter, T. Ziebart, S. Grimm, D. Meila, E. Krieger, and H. Wehrbein, *Induction of IL-6 and MMP-8 in human periodontal fibroblasts by static tensile strain.* Clin Oral Investig, 2014. **18**(3): p. 901-8.
70. Proskuryakov, S.Y.a., A.G. Konoplyannikov, and V.L. Gabai, *Necrosis: a specific form of programmed cell death?* Experimental Cell Research, 2003. **283**(1): p. 1-16.
71. Väyrynen, J.P., J. Vornanen, T. Tervahartiala, T. Sorsa, R. Bloigu, T. Salo, A. Tuomisto, and M.J. Mäkinen, *Serum MMP-8 levels increase in colorectal cancer and correlate with disease course and inflammatory properties of primary tumors.* International Journal of Cancer, 2012. **131**(4): p. E463-E474.
72. Tominaga, M., S. Tengara, A. Kamo, H. Ogawa, and K. Takamori, *Matrix metalloproteinase-8 is involved in dermal nerve growth: Implications for possible application to pruritus from in vitro models.* J Invest Dermatol, 2011. **131**(10): p. 2105-12.
73. Vartak, D.G. and R.A. Gemeinhart, *Matrix metalloproteases: Underutilized targets for drug delivery.* Journal of drug targeting, 2007. **15**(1): p. 1-20.
74. Fingleton, B., *MMPs as therapeutic targets – still a viable option?* Seminars in cell & developmental biology, 2008. **19**(1): p. 61-68.

75. Bode, W., P. Reinemer, R. Huber, T. Kleine, S. Schnierer, and H. Tschesche, *The X-ray crystal structure of the catalytic domain of human neutrophil collagenase inhibited by a substrate analogue reveals the essentials for catalysis and specificity.* The EMBO Journal, 1994. **13**(6): p. 1263-1269.

76. Lu, K.G. and C.M. Stultz, *Insight into the degradation of type-I collagen fibrils by MMP-8.* Journal of Molecular Biology, 2013. **425**(10): p. 1815-1825.

77. Babine, R.E. and S.L. Bender, *Molecular recognition of protein−ligand complexes: applications to drug design.* Chemical Reviews, 1997. **97**(5): p. 1359-1472.

78. Schechter, I. and A. Berger, *On the size of the active site in proteases. I. Papain.* Biochem Biophys Res Commun, 1967. **27**(2): p. 157-62.

79. Gupta, S.P. and V.M. Patil, *Specificity of binding with matrix metalloproteinases.* Exs, 2012. **103**: p. 35-56.

80. Mei, M.L., Q.L. Li, C.H. Chu, C.K. Yiu, and E.C. Lo, *The inhibitory effects of silver diamine fluoride at different concentrations on matrix metalloproteinases.* Dent Mater, 2012. **28**(8): p. 903-8.

81. Chu, C.H., E.C. Lo, and H.C. Lin, *Effectiveness of silver diamine fluoride and sodium fluoride varnish in arresting dentin caries in Chinese pre-school children.* J Dent Res, 2002. **81**(11): p. 767-70.

82. Lo, E.C., C.H. Chu, and H.C. Lin, *A community-based caries control program for pre-school children using topical fluorides: 18-month results.* J Dent Res, 2001. **80**(12): p. 2071-4.

83. Yee, R., C. Holmgren, J. Mulder, D. Lama, D. Walker, and W. van Palenstein Helderman, *Efficacy of silver diamine fluoride for Arresting Caries Treatment.* J Dent Res, 2009. **88**(7): p. 644-7.

84. Zhou, X., J. Lu, D. Chen, W. Wang, Q. Cai, T. Li, and J. Zhang, *Matrix metalloproteinase-8 inhibitors mitigate sepsis-induced myocardial injury in rats.* Chin Med J (Engl), 2014. **127**(8): p. 1530-5.

85. Harkness, K.A., P. Adamson, J.D. Sussman, G.A.B. Davies-Jones, J. Greenwood, and M.N. Woodroofe, *Dexamethasone regulation of matrix metalloproteinase expression in CNS vascular endothelium.* Brain, 2000. **123**(4): p. 698-709.

86. Bian, F., F.S.A. Pelegrino, J.T. Henriksson, S.C. Pflugfelder, E.A. Volpe, D.-Q. Li, and C.S. de Paiva, *Differential effects of dexamethasone and doxycycline on inflammation and MMP production in murine alkali-burned corneas associated with dry eye.* The Ocular Surface, 2016. **14**(2): p. 242-254.

87. Ong, C.W., P.T. Elkington, S. Brilha, C. Ugarte-Gil, M.T. Tome-Esteban, L.B. Tezera, P.J. Pabisiak, R.C. Moores, T. Sathyamoorthy, V. Patel, R.H. Gilman, J.C. Porter, and J.S. Friedland, *Neutrophil-derived MMP-8 drives AMPK-dependent matrix destruction in human pulmonary tuberculosis.* PLoS Pathog, 2015. **11**(5): p. e1004917.

88. Hanemaaijer, R., H. Visser, P. Koolwijk, T. Sorsa, T. Salo, L.M. Golub, and V.W. van Hinsbergh, *Inhibition of MMP synthesis by doxycycline and chemically modified tetracyclines (CMTs) in human endothelial cells.* Adv Dent Res, 1998. **12**(2): p. 114-8.

89. Choi, D.H., I.S. Moon, B.K. Choi, J.W. Paik, Y.S. Kim, S.H. Choi, and C.K. Kim, *Effects of sub-antimicrobial dose doxycycline therapy on crevicular fluid MMP-8, and gingival tissue MMP-9, TIMP-1 and IL-6 levels in chronic periodontitis.* J Periodontal Res, 2004. **39**(1): p. 20-6.

90. Smith, G.N., Jr., E.A. Mickler, K.A. Hasty, and K.D. Brandt, *Specificity of inhibition of matrix metalloproteinase activity by doxycycline: relationship to structure of the enzyme.* Arthritis Rheum, 1999. **42**(6): p. 1140-6.

91. Gendron, R., D. Grenier, T. Sorsa, and D. Mayrand, *Inhibition of the activities of matrix metalloproteinases 2, 8, and 9 by chlorhexidine.* Clin Diagn Lab Immunol, 1999. **6**(3): p. 437-9.

92. Teronen, O., Y.T. Konttinen, C. Lindqvist, T. Salo, T. Ingman, A. Lauhio, Y. Ding, S. Santavirta, and T. Sorsa, *Human neutrophil collagenase MMP-8 in peri-implant sulcus fluid and its inhibition by clodronate.* J Dent Res, 1997. **76**(9): p. 1529-37.

93. Gerlt, J.A. and P.C. Babbitt, *Divergent evolution of enzymatic function: Mechanistically diverse superfamilies and functionally distinct suprafamilies.* Annual Review of Biochemistry, 2001. **70**(1): p. 209-246.

94. Betz, M., P. Huxley, S.J. Davies, Y. Mushtaq, M. Pieper, H. Tschesche, W. Bode, and F.X. Gomis-Ruth, *1.8-A crystal structure of the catalytic domain of human neutrophil collagenase (matrix metalloproteinase-8) complexed with a peptidomimetic hydroxamate*

primed-side inhibitor with a distinct selectivity profile. Eur J Biochem, 1997. **247**(1): p. 356-63.

95. Brandstetter, H., F. Grams, D. Glitz, A. Lang, R. Huber, W. Bode, H.-W. Krell, and R.A. Engh, *The 1.8-Å crystal structure of a matrix metalloproteinase 8-barbiturate inhibitor complex reveals a previously unobserved mechanism for collagenase substrate recognition.* Journal of Biological Chemistry, 2001. **276**(20): p. 17405-17412.
96. Demeestere, D., E. Dejonckheere, S. Steeland, P. Hulpiau, J. Haustraete, N. Devoogdt, R. Wichert, C. Becker-Pauly, E. Van Wonterghem, S. Dewaele, G. Van Imschoot, J. Aerts, L. Arckens, Y. Saeys, C. Libert, and R.E. Vandenbroucke, *Development and validation of a small single-domain antibody that effectively inhibits matrix metalloproteinase 8.* Mol Ther, 2016.
97. Chames, P., M. Van Regenmortel, E. Weiss, and D. Baty, *Therapeutic antibodies: successes, limitations and hopes for the future.* British Journal of Pharmacology, 2009. **157**(2): p. 220-233.
98. Pisal, D.S., M.P. Kosloski, and S.V. Balu-Iyer, *Delivery of therapeutic proteins.* Journal of pharmaceutical sciences, 2010. **99**(6): p. 2557-2575.
99. Bae, Y.H. and K. Park, *Targeted drug delivery to tumors: Myths, reality and possibility.* Journal of Controlled Release, 2011. **153**(3): p. 198-205.
100. Pasut, G. and F.M. Veronese, *State of the art in PEGylation: The great versatility achieved after forty years of research.* Journal of Controlled Release, 2012. **161**(2): p. 461-472.
101. Podust, V.N., S. Balan, B.-C. Sim, M.P. Coyle, U. Ernst, R.T. Peters, and V. Schellenberger, *Extension of in vivo half-life of biologically active molecules by XTEN protein polymers.* Journal of Controlled Release.
102. Dixit, N., P. Spencer, and J.S. Laurence, *Protein-polymeric materials interaction: mineralized tissues reconstruction*, in *Encyclopedia of Biomedical Polymers and Polymeric Biomaterials*. 2015, Taylor & Francis. p. 6808-6830.
103. Tjaderhane, L., H. Larjava, T. Sorsa, V.J. Uitto, M. Larmas, and T. Salo, *The activation and function of host matrix metalloproteinases in dentin matrix breakdown in caries lesions.* J Dent Res, 1998. **77**(8): p. 1622-9.

104. Chaussain-Miller, C., F. Fioretti, M. Goldberg, and S. Menashi, *The role of matrix metalloproteinases (MMPs) in human caries.* J Dent Res, 2006. **85**(1): p. 22-32.

105. Seseogullari-Dirihan, R., F. Apollonio, A. Mazzoni, L. Tjaderhane, D. Pashley, L. Breschi, and A. Tezvergil-Mutluay, *Use of crosslinkers to inactivate dentin MMPs.* Dent Mater, 2016. **32**(3): p. 423-32.

106. Dixit, N., J.K. Settle, Q. Ye, C.L. Berrie, P. Spencer, and J.S. Laurence, *Grafting MAP peptide to dental polymer inhibits MMP-8 activity.* J Biomed Mater Res B Appl Biomater, 2015. **103**(2): p. 324-31.

107. Tucker, J.K., M.L. McNiff, S.B. Ulapane, P. Spencer, J.S. Laurence, and C.L. Berrie, *Mechanistic investigations of matrix metalloproteinase-8 inhibition by metal abstraction peptide.* Biointerphases, 2016. **11**(2): p. 021006.

108. McNiff, M.L., E.P. Haynes, N. Dixit, F.P. Gao, and J.S. Laurence, *Thioredoxin fusion construct enables high-yield production of soluble, active matrix metalloproteinase-8 (MMP-8) in Escherichia coli.* Protein Expr Purif, 2016. **122**: p. 64-71.

109. Krause, M.E., A.M. Glass, T.A. Jackson, and J.S. Laurence, *Novel tripeptide model of nickel superoxide dismutase.* Inorg Chem, 2010. **49**(2): p. 362-4.

CHAPTER 2.
MMP-8 CONDITION OPTIMIZATION FOR HIGH-RESOLUTION SOLUTION NMR ANALYSIS OF ENZYME STABILITY AND INHIBITOR INTERACTIONS

2.1 INTRODUCTION

Matrix metalloproteinase (MMP)-8 plays an important role in the development and progression of several inflammatory diseases, such as periodontitis, asthma, and rheumatoid arthritis. Through regulation of inflammatory mediators, MMP-8 causes increased inflammation and worsening of disease state, and the mechanisms by which it participates in disease progression are discussed in detail in Chapter 1. Because of its destructive role in activating key pathways, it is strongly believed that inhibition of MMP-8 would reduce inflammation in patients with these conditions and lead to better disease management and prognosis. Several MMP-8 inhibitors have been tested in cell culture and rat models, and some of these compounds also have been tested in the clinic to control inflammatory diseases, such as periodontitis. However, the mechanism of inhibition is not always known.

Understanding the mechanism by which inhibition is accomplished is important for drug discovery and development in order to obtain the most desirable therapeutic outcome, especially for drugs that affect targets involved in multiple pathways and functions in the body. Inhibitors can interact with an enzyme and prevent enzymatic function for different lengths of time, influenced by inhibitor size and binding efficiency, which alters the amount of inhibitor needed to achieve the desired level of inhibition [1]. Knowing more information about the structure of MMP-8, where an inhibitor can bind to the enzyme, and how the inhibitor impedes enzymatic action will contribute to the understanding of the methods of inhibitor interaction with this important drug target and will allow for further development of more selective and effective inhibitors.

As a member of the MMP family, MMP-8 is difficult to express because its proteolytic activity leads to autoproteolysis [2]. Preparing the protein as a thioredoxin (Trx)-MMP-8 fusion construct improves the stability of MMP-8, which allows for high-yield protein production and enables analysis [3]. Trx helps maintain the folded protein structure by a yet known mechanism and improves the stability of MMP-8 by folding with and preventing cleavage of MMP-8 [4]. The longer lifetime of MMP-8 is required to conduct more detailed structural and biophysical analyses such as three-dimensional (3D) nuclear magnetic resonance (NMR) experiments.

High-resolution solution NMR is an important tool in the pharmaceutical industry to understand protein-drug interactions [5]. Tracking perturbations in the physical properties of the protein provides information about protein structure, mechanism of binding, and kinetics of the binding interaction. To track these changes, two-dimensional (2D) ^{1}H-^{15}N heteronuclear single quantum coherence (HSQC) experiments are used to show connectivity between nuclei [6]. In the repeating nature of a protein's primary sequence, a series of NH groups from the amino acids composing the protein sequence are connected through amide bonds and each becomes chemically unique when embedded in the protein's tertiary structure. The ^{1}H-^{15}N HSQC experiment detects only protons directly coupled to nitrogen [7], and the spectrum displays one cross peak at the position of the ^{1}H and ^{15}N chemical shifts for each amide in the protein backbone [8].

A fingerprint of the protein is created from the HSQC experiment and allows for tracking ligand binding, protein behavior, and protein folding [5]. Alterations in the physical or chemical environment of an amino acid result in changes in the ^{1}H and ^{15}N NMR chemical shifts. Protein folding imposes unique structural constrains that affect chemical shift positions, distinguishing the spectra of folded proteins from unstructured molecules or unfolded proteins. When a protein

is unfolded, losing its secondary and tertiary structure, the chemical shift distribution for the amino acids collapses into a narrow proton ppm range similar to that of small molecule compounds which have no preferred orientation and undergo rapid, random motions that average on the NMR timescale [9]. When a ligand binds to a protein, the electronic shielding, hence magnetic susceptibility, of affected nuclei changes, and perturbations to the backbone amide chemical shifts are detected [5, 10]. The protein's sequential backbone resonance assignments, which can be determined through 3D NMR experiments, can be directly tied to the HSQC data, allow for determination of the residues involved in ligand binding and provide a basis for understanding the inhibition mechanism. In theory, HSQC experiments can be used to track amino acid perturbations of MMP-8 from the addition of inhibitors, and correlating the HSQC data with the backbone assignments will provide information about where the protein inhibitor interaction occurs. Although the crystal structure of MMP-8 was reported previously [11-13], the NMR backbone assignments have not yet been determined, and obtaining these assignments would help in the determination of the mechanism of MMP-8 inhibition.

Inhibitors of enzyme catalytic activity can interact with proteins through various mechanisms. The protein inhibitor interactions can be reversible or irreversible and competitive, uncompetitive, or non-competitive, and inhibition can be accomplished through direct inhibition, allosteric inhibition, direct binding with catalytic ions, or through chelation of the catalytic ions [14]. The mechanism of inhibition is unknown for several of the MMP-8 inhibitors that have been tested, and understanding the mechanism of protein inhibitor interaction would provide useful information for the development of more effective inhibitors. Investigating a mechanism of MMP-8 inhibition, recent studies have demonstrated the interaction of MMP-8 with a metal binding peptide, NCC, with the goal of preventing dental composite failures from dentin

degradation by MMP-8 [15, 16]. NCC, a metal abstraction peptide (MAP) with the amino acid sequence Asn-Cys-Cys, tightly binds transition metals and has been investigated as a method to target metal delivery for treatment and diagnosis of diseases [17]. Although the mechanism of interaction has not been confirmed, NCC, when chemically conjugated to 2-aminoethyl methacrylate hydrochloride (AEMA) containing dental polymers, is thought to bind to the catalytic Zn^{2+} ion in the MMP-8 active site and is a potent inhibitor of the protein enzymatic activity [16]. In additional studies using self-assembled monolayers (SAMs), NCC directly interacted with MMP-8 through the catalytic Zn^{2+} ion in the active site [15]. NCC has high affinity for MMP-8 and is a very slowly reversible inhibitor of enzymatic action. With the information from these previous studies, the goal of this project was to determine resonance assignments for the protein backbone of MMP-8 using multi-dimensional heteronuclear solution NMR and then to use the assignments to study the mechanism of inhibitor interaction to aid in the development of more potent and selective MMP-8 inhibitors.

2.2 METHODS

2.2.1 Protein Expression and Purification

Expression and purification of MMP-8 was completed as previously described using a fusion construct with an N-terminal thioredoxin tag (Trx-MMP-8 fusion) [3]. The plasmid for Trx-MMP-8 fusion protein was transformed into BL21 *Escherichia coli* cell strain using the standard heat shock method. The cells were incubated overnight at 37 ^{o}C with 100 μg/mL ampicillin. To prepare ^{15}N-labeled and ^{13}C, ^{15}N-labeled cultures, individual colonies were inoculated in 50 mL M9ZB media, prepared with ammonium-^{15}N chloride, supplemented with 0.4% glucose, 1 mM $MgSO_4$, and 100 μg/mL ampicillin. The starter cultures were grown for 16 h at 37 ^{o}C in an orbital shaker at 250 rpm. Thirty milliliters of the ^{15}N-labeled cultures was

transferred to 1 L minimal media containing trace minerals and minimal salts [18]. Thirty milliliters of the ^{13}C, ^{15}N-labeled cultures was added to inoculate 1 L minimal media containing trace minerals and minimal salts and supplemented with ^{13}C-glucose. The ^{15}N-labeled and ^{13}C, ^{15}N-labeled media cultures were incubated at 37 ^{o}C and 250 rpm until the OD_{600} reached approximately 0.7. With the addition of 1 mM isopropyl β-D-1-thiogalactopyranoside (IPTG), protein expression was induced. After incubating for 4 h at 37 ^{o}C and 250 rpm, the cells were harvested by centrifugation for 8 min at 3,600 x g and 4 ^{o}C. Cell pellets were stored at -80 ^{o}C until use.

To purify MMP-8, each pellet (from 1L of culture) was resuspended in 25 mL lysis buffer (50 mM Tris-HCl, 60 mM NaCl, 20 mM imidazole, pH 7.9) and lysed using three passes through a French Press at 21,000 psi. Cell lysates were centrifuged at 21,000 x g for 1 h at 4 ^{o}C, and the supernatant, which contained the protein, was filtered through 0.45 μm filter followed by a 0.2 μm filters to remove cellular debris. The protein containing sample was applied to a 5 mL Hi-Trap Chelating HP column (GE Lifesciences) charged with nickel and equilibrated in lysis buffer. To remove cellular proteins, the column was washed with 10 column volumes (CV) of wash buffer (50 mM Tris-HCl, 60 mM NaCl, 40 mM imidazole, pH 7.9) at a flow rate of 1.25 mL/min at 4 ^{o}C. The protein was eluted from the column using a linear gradient from 0 to 100% elution buffer (50 mM Tris-HCl, 60 mM NaCl, 500 mM imidazole, pH 7.9). The protein containing elution fractions were concentrated using an Amicon Ultra 10 kDa MWCO concentrator (Millipore) to approximately 0.6-1.5 mM. The sample was dialyzed in 1 L dialysis buffer (50 mM Tris-HCl, 60 mM NaCl, pH 7.9) at room temperature for 1 h in a 10 kDa MWCO dialysis cassette followed by 1 h dialysis in fresh 1 L dialysis buffer to remove imidazole. Purified samples were stored at 4 ^{o}C until ready to analyze.

2.2.2 SDS-PAGE Analysis

SDS-PAGE samples were prepared by mixing 30 μL of sample with an equal volume of reducing Laemmli buffer and were heated for 10 min at 90 ^{o}C before loading onto the gel. Gel samples were loaded onto standard 4% (v/v) stacking, 15% (v/v) resolving gels and run at 135 V for 2 h and referenced to a prestained, dual-color molecular weight marker (BioRad, #161-0374). Gels were stained with Coomassie (R-250) for visualization of protein molecular weight.

2.2.3 NMR Experiments

All NMR experiments were carried out at 25 ^{o}C using a Bruker Avance 800 MHz NMR spectrometer using a cryogenic, triple-resonance probe equipped with pulse field gradients. To optimize sample conditions, 0.3 mM ^{15}N-labeled MMP-8 protein samples were prepared in 50 mM Tris-HCl, 60 mM NaCl, pH 8.5, with 5% D_2O, unless otherwise noted. Bradford assay was used to check the sample concentrations before analysis. Two-dimensional ^{1}H-^{15}N HSQC spectra were collected in 8 scans with 2048 points in the ^{1}H dimension and 180 points in the ^{15}N dimension. HSQC spectra were processed using NMRPipe [19] and analyzed with Sparky [20].

For collection of peak assignment data, 3D versions of HNCACB and CBCA(CO)NH experiments were obtained and referenced to the 2D ^{1}H-^{15}N HSQC spectra. The HNCACB was acquired in 96 scans with 2048, 32, and 110 points in the ^{1}H, ^{15}N, and ^{13}C dimensions, respectively. The CBCA(CO)NH experiment was collected in 32 scans with 2048, 56, and 176 points in the ^{1}H, ^{15}N, and ^{13}C dimensions, respectively. For the 3D NMR samples, 0.3 mM ^{15}N-^{13}C-labeled MMP-8 protein was incubated with 0.6 mM NCC peptide in 50 mM Tris-HCl, 60 mM NaCl, pH 8.5 on a laboratory nutator at 20 rpm for 2 h at room temperature. The incubation samples were then concentrated to 1.0 mM MMP-8 using Amicon Ultra 30 kDa MWCO concentrator (Millipore) and dialyzed in 50 mM Tris-HCl, 60 mM NaCl, pH 8.5 to

remove excess, unbound NCC peptide. NMR samples were prepared as 1.0 mM ^{15}N-^{13}C MMP-8 plus bound NCC, 50 mM Tris-HCl, 60 mM NaCl, pH 8.5, with 5% D_2O. The 3D NMR data was processed using NMRPipe [19] and analyzed in NMR View [21].

2.3 RESULTS

2.3.1 pH Titrations

Initial ^{1}H-^{15}N HSQC experiments were performed and the solution conditions of the protein sample varied to optimize the quality of the 2D spectrum. Because ^{1}H-^{15}N HSQC experiments look at the NH bond of the amino acid backbone, Tris is not the most favorable buffer because it also has a NH bond, which may produce additional signal in the spectra that may interfere with the data. To avoid this complication, lower pH titrations were performed with 0.3 mM ^{15}N MMP-8 in 50 mM sodium phosphate. Overlay of the spectra at various pH (7.9, 7.7, 7.4, and 7.2) is shown in Figure 2.1. As the pH of the sample is lowered from 7.9 to 7.2, the

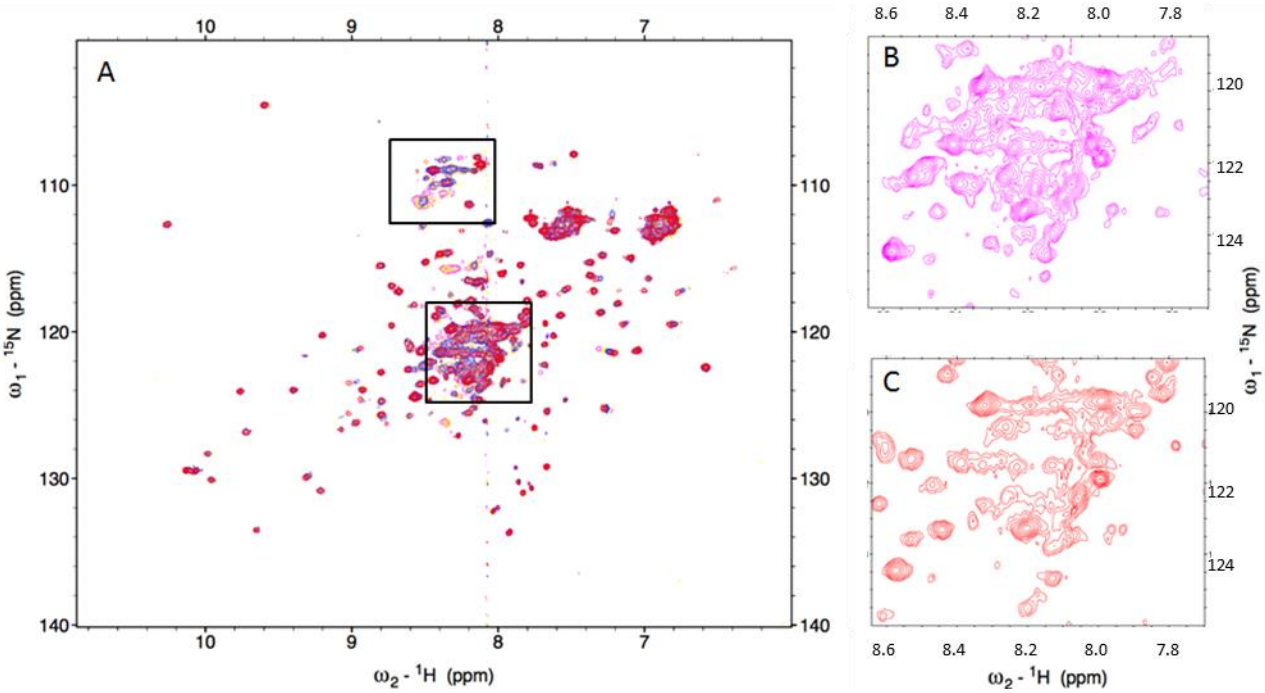

Figure 2.1 ^{1}H-^{15}N HSQC spectra of MMP-8 pH titration. Sample of 0.3 mM MMP-8 in 50 mM Sodium Phosphate at pH 7.9 (red), 7.7 (blue), 7.4 (yellow), and 7.2 (pink) shown (A). The tertiary structure of the protein is similar at each pH, but better resolution is observed for some regions of peaks at higher pH (boxed). Zoomed in spectra of pH 7.2 (B) and pH 7.9 (C) show the difference in resolution in the central boxed region.

more structured, outer peaks from the folded protein decrease in intensity, and the center unstructured region is more crowded, which suggests MMP-8 either is unfolding or the structured portion is self-associating to form unobservable oligomeric species while the unstructured portions of the fusion protein remain visible. As the pH was lowered further to 6.8 and incrementally reduced to pH 4.0, NMR signal was lost rapidly as MMP-8 precipitated out of solution, presumably due to decreased solubility near the protein's isoelectric point. All the protein was recovered in a soluble folded form as the pH was lowered further to pH 3.0. Sodium acetate (7.4 mM) was added to the pH 3.0 sample to accomplish buffering. Figure 2.2 shows more well-resolved peaks and improved peak resolution in the central region of the spectrum at pH 3.0.

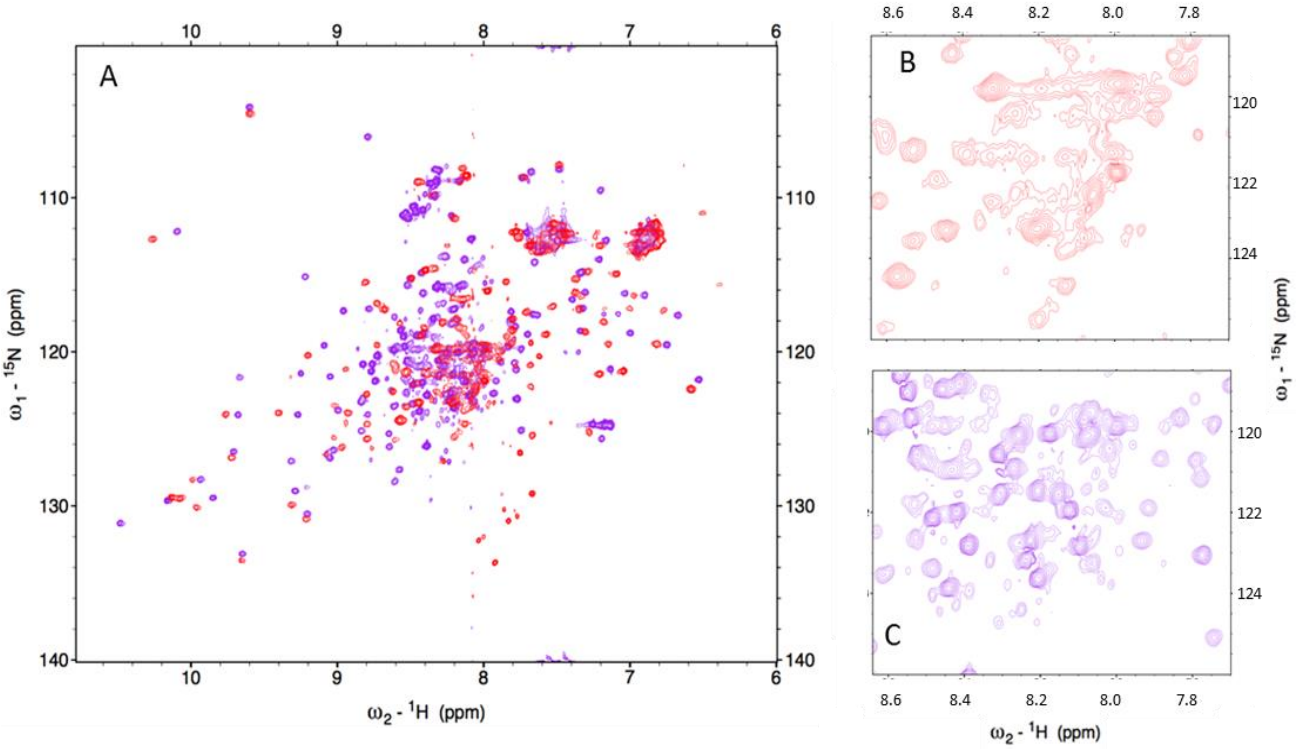

Figure 2.2 ^{1}H-^{15}N HSQC spectra comparing MMP-8 at pH 7.9 and pH 3.0. A Sample of 0.3 mM MMP-8 in 50 mM Sodium Phosphate, 7.4 mM Sodium Acetate, pH 7.9 (red) and pH 3.0 (purple) shown (A). At pH 3.0, more peaks and better resolution are observed throughout the spectra. Fewer peaks and worse resolution are observed in the central region of the spectra at pH 7.9 (B) than at pH 3.0 (C).

Titrations at high pH also were carried out in increments of 0.1 pH unit from pH 7.9 to 8.5 with 0.3 mM ^{15}N MMP-8, 50 mM Tris-HCl, 60 mM NaCl. Overlaid spectra of pH titration points indicate that resolution of MMP-8 peaks improves with increasing pH (Figure 2.3). Unfortunately, chemical exchange of HN protons with the aqueous solvent at basic pH can lead to loss of signals in the NMR spectrum. As such, no condition was identified in which the expected number of peaks for the entire protein molecule was observed. There are 323 residues in the fusion construct, 120, 32, and 152 non-proline residues in Trx, the linker and MMP-8, respectively. Under the best condition of 50 mM Tris-HCl, 60 mM NaCl, pH 8.5, 195 peaks were observed, which represents 60% of the fusion sequence. This number of peaks is larger than Trx and the linker combined, indicating that at least some portion of the peaks must

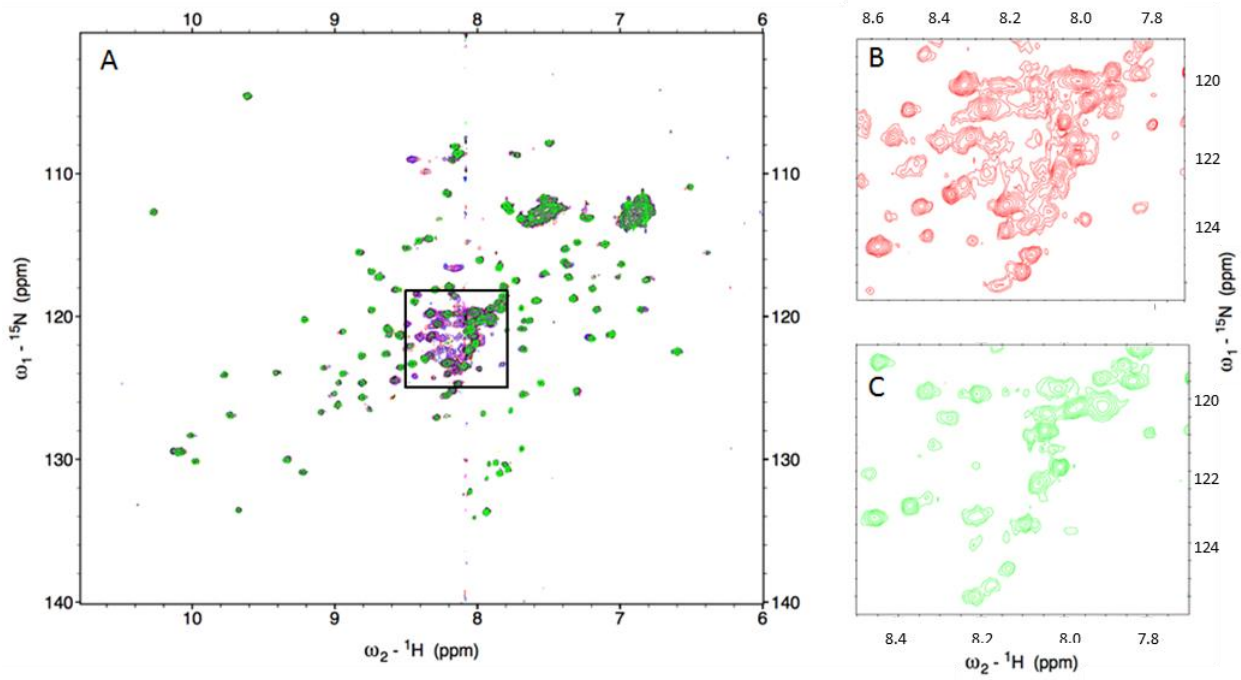

Figure 2.3 ^{1}H-^{15}N HSQC spectra of MMP-8 high pH titration. Sample of 0.3 mM MMP-8 in 50 mM Tris-HCl, 60 mM NaCl at pH 7.9 (red), 8.0 (blue), 8.1 (yellow), 8.2 (pink), 8.3 (purple), 8.4 (black), 8.5 (green) shown (A). The tertiary structure of the protein is similar at each pH, but better resolution is observed for central regions of peaks at higher pH (boxed). Zoomed in spectra of pH 7.9 (B) and pH 8.5 (C) show the improved resolution at higher pH in the central boxed region. The pH increases may affect the chemical exchange, which could cause the loss of some signals.

correspond to MMP-8. The spectra were compared to that of Trx alone to determine if most peaks were from Trx or a mixture of MMP-8 and Trx. Clear differences were observed in the regions of the spectrum that correspond to unique well-folded portions of the Trx protein. Based on the spectral differences, it was anticipated that the peaks reflected at least some structured portion of both entities from the fusion construct.

2.3.2 Effect of metal ions

Further structural improvements of MMP-8 were observed with the addition of excess Ca^{2+} and Zn^{2+} ions. A 0.6 mM ^{15}N MMP-8, 50 mM Tris-HCl, 60 mM NaCl, pH 7.9 sample was dialyzed in 10 mM Tris base, 7.4 mM sodium acetate, 5 mM $CaCl_2$, 20 μM $ZnCl_2$, pH 7.9. When the MMP-8 sample was dialyzed with excess metal ions at pH 7.9, white precipitates formed, indicating that the protein precipitated out of solution, but MMP-8 was soluble again when the pH was titrated down to 3.0. When analyzed by ^{1}H-^{15}N HSQC, the sample had improved peak shape in the presence of the added metal ions compared to the sample at the same pH without excess metal ions (Figure 2.4A). The metal ions resulted in peaks with reduced widths at half height by approximately 20%, making the peaks sharper and better resolved.

When further investigated, a MMP-8 sample with excess Ca^{2+} but not excess Zn^{2+} showed similar structure as compared to the protein without any excess ions (Figure 2.4B). Removal of all ions, through dialysis at low pH, resulted in migration of peaks toward the center of the HSQC spectra, which indicates loss of protein structure and transition to an unfolded protein (Figure 2.4C). The loss of structured protein peaks in the outer regions of the spectrum after removing the metal ions suggests the tertiary structure of MMP-8 is dependent on binding the zinc ion. The structure of the protein without metal ions was mostly restored after overnight incubation with excess Ca^{2+} (5 mM $CaCl_2$) and Zn^{2+} (20 μM $ZnCl_2$) ions (Figure 2.4D). The

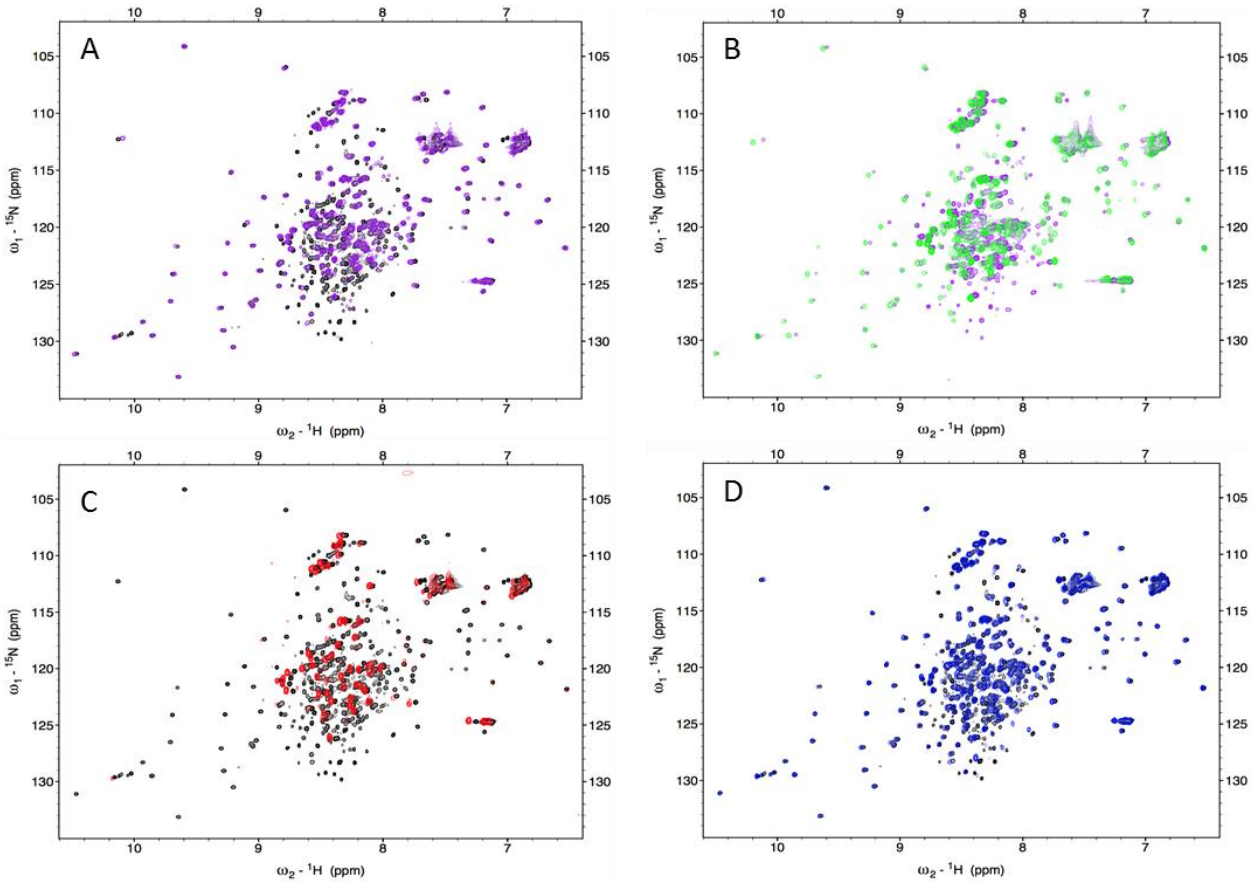

Figure 2.4 ^{1}H-^{15}N HSQC spectra of MMP-8 with metal ions. Comparison of sample of 0.6 mM MMP-8 in 10 mM Tris base, 5 mM $CaCl_2$, 20 μM $ZnCl_2$, pH 3.0 (black) to samples with varying amounts of metal ions. (A) The addition of excess Ca^{2+} and Zn^{2+} ions (black) improves the MMP-8 structure and resolution of the spectral peaks compared to the spectrum when no excess metal ions are added (purple). (B) Excess Ca^{2+} ions only (green) do effect the structure slightly through peak shifting, but the Ca^{2+} ions do not affect the structure as significantly as when the Zn^{2+} ions are also present. (C) When all the ions are dropped out of MMP-8 (red), the protein structure is lost, as seen with the reduced number of peaks. (D) After incubation with excess Ca^{2+} and Zn^{2+} (blue), MMP-8 structure is mostly restored, as the blue and black peaks mostly overlap.

affinities of the metal ions to MMP-8 have not been determined, but for comparison, MMP-26 has one high-affinity and one low-affinity Ca^{2+} binding site with dissociation constants of 62.9 nM and 120 μM, respectively, at pH 7.5 [22]. It was not determined how much residual zinc or calcium was present in the purified protein sample, but both calcium-binding sites should be occupied fully in the presence of 5 mM $CaCl_2$. To my knowledge, no data is available for any

MMP on the zinc binding constant. At lower pH, the metal ion affinities will decrease, but the addition of excess metal ion will allow for restoration of the ion binding to MMP-8.

2.3.3 Inhibitor Effects

Initial inhibitor studies were investigated using 0.2 mM ^{15}N MMP-8 in 50 mM sodium phosphate, 7.4 mM sodium acetate, pH 3.0. NNGH, a known inhibitor of MMPs [23], was dissolved in DMSO and added to the protein sample in a molar ratio of 19:1 NNGH:MMP-8. Several distinct changes were observed in the HSQC of the NNGH-containing sample compared to the protein alone. Due to the limited solubility of NNGH in aqueous solution, the resulting sample contained 3.4% DMSO. Comparison with a control sample (prepared with the same protein sample conditions and amount of DMSO, without NNGH) indicated that the changes observed in the ^{1}H-^{15}N HSQC spectra were entirely due to the impact of DMSO on MMP-8 structure and obscured any more subtle effect of the NNGH interaction with MMP-8, making inhibitor specific changes difficult to determine (Figure 2.5). The sample was subsequently prepared using 1.0% DMSO, but there was not sufficient improvement in the data to permit analysis of the inhibitor binding effect on MMP-8. Further reduction by a meaningful amount in the percent solvent was not possible without also substantially decreasing the amount of NNGH in the sample. Addition of 3.4% and 1.0% DMSO to the buffer only (10 mM Tris base, 5 mM $CaCl_2$, 20 μM $ZnCl_2$, pH 3.0) caused the metal ions to precipitate out of solution. The addition of DMSO caused more changes to the protein sample and buffer conditions than the presence of NNGH inhibitor, and as such, this line of investigation was terminated.

Because of the negative impact to protein structure from the addition of DMSO, it became evident that water-soluble inhibitors are necessary to study inhibitor interactions with MMP-8 by solution NMR. NCC, a metal binding tripeptide, was investigated as a MMP-8

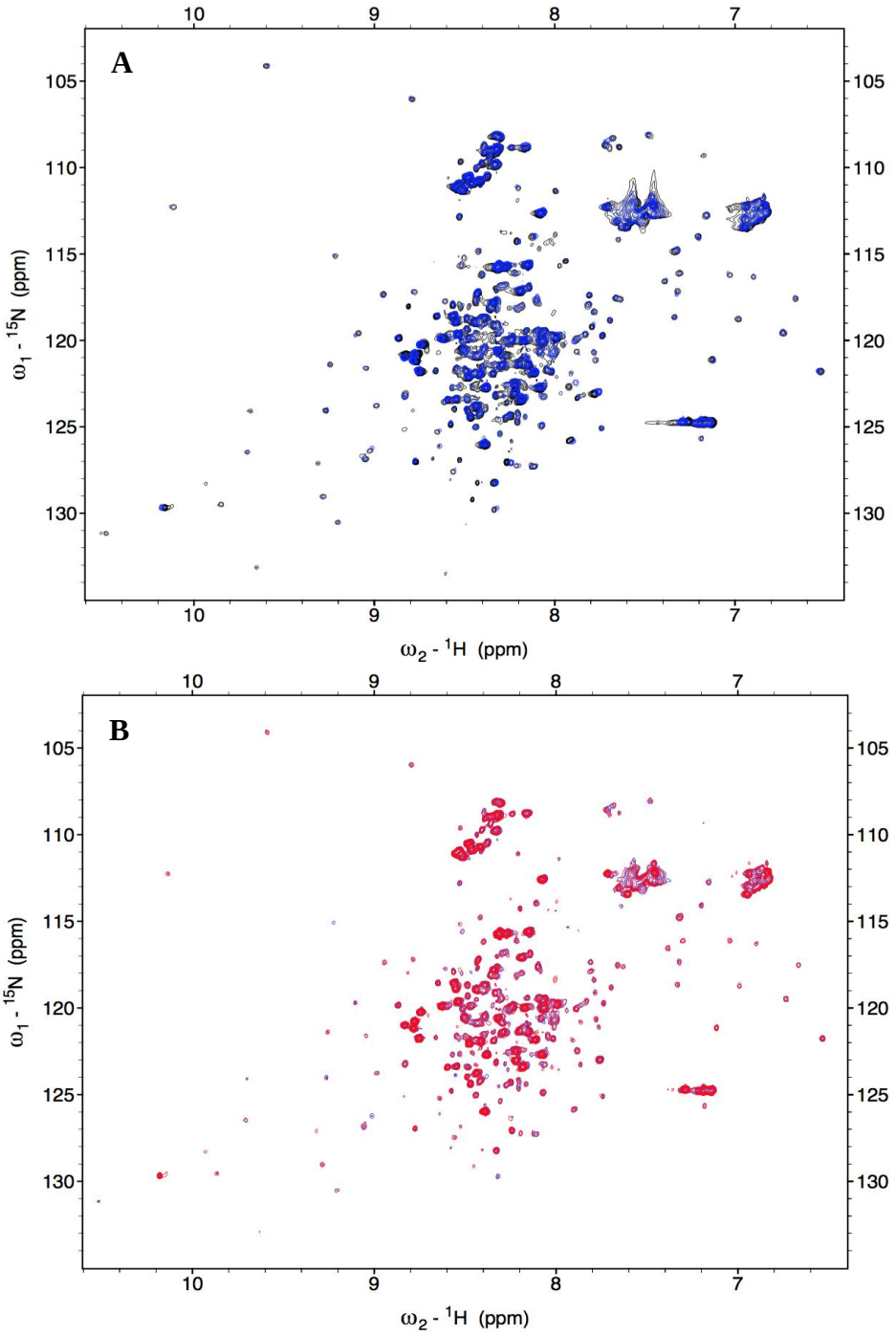

Figure 2.5 ^{1}H-^{15}N HSQC spectra of MMP-8 with NNGH and DMSO. (A) Sample of 0.2 mM ^{15}N MMP-8 in 50 mM sodium phosphate, 7.4 mM sodium acetate, pH 3.0 (black) compared with samples of same conditions and 19:1 NNGH to MMP-8, 3.4% DMSO (blue) shows several spectral perturbations. (B) Comparison of 19:1 NNGH to MMP-8, 3.4% DMSO (blue) to a control sample with MMP-8 only, 3.4% DMSO (red) shows a similar HSQC spectrum. The tertiary structure of MMP-8 is significantly different with the addition of DMSO, through the missing and loss of intensity of several peaks. Inhibitor interaction with MMP-8 was not apparent since no differences were observed between the spectra of the control and NNGH.

inhibitor. NCC has been shown to interact with and bind to MMP-8, and it is proposed to bind 1:1 to the Zn^{2+} ion in the MMP-8 active site [15, 16]. NCC was slowly titrated into 0.3 mM ^{15}N MMP-8, 10 mM Tris base, 7.4 mM sodium acetate, 5 mM $CaCl_2$, 20 μM $ZnCl_2$, pH 3.0 in 0.3 mM NCC increments. Based on previous studies, binding of NCC to MMP-8 qualitatively seems to occur on the scale of many minutes to a few hours and is reversible on a longer time scale. Because the mechanism of binding has not been elucidated fully and the rate to reach equilibrium or saturation has not been determined, the samples were incubated at 4:1 NCC to MMP-8 for 21.5 h to maximize interaction between the inhibitor and MMP-8. Comparison of the ^{1}H-^{15}N HSQC data show no detectable differences that would indicate a structural change has occurred to MMP-8 when incubated with excess NCC at low pH (Figure 2.6A). This is in agreement with previous studies. Studies using Ni^{2+} ions show NCC releases bound metals at neutral to low pH [24] and ellipsometry studies using NCC-grafted SAMS show that native, Zn-bound MMP-8 is released from the surface at pH 3.5 [15]. As such, investigation of NCC interaction with NCC was conducted at basic pH.

The NMR spectra of MMP-8 were observed to improve upon increasing the sample pH to 8.5 (section 2.3.1), and higher pH allowed for NCC interaction with MMP-8 (Figure 2.6B). Two peaks at approximately 8.8 ppm in the ^{1}H dimension and 125 ppm in the ^{15}N dimension begin to appear and increase in intensity when MMP-8 is incubated with NCC in a 2:1 NCC to MMP-8 ratio. Peaks at approximately 8.6 ppm in ^{1}H and 118 ppm in ^{15}N and in the region of 7.8-8.0 ppm in the ^{1}H dimension and 123-127 ppm in the ^{15}N dimension also begin to appear with the addition of NCC. With only a few changes in the ^{1}H-^{15}N HSQC spectrum, the data indicate MMP-8 is interacting with NCC and suggest that NCC is binding to the enzyme in a single, localized region. Because only a subset of MMP-8 residues is represented in the spectrum, it also

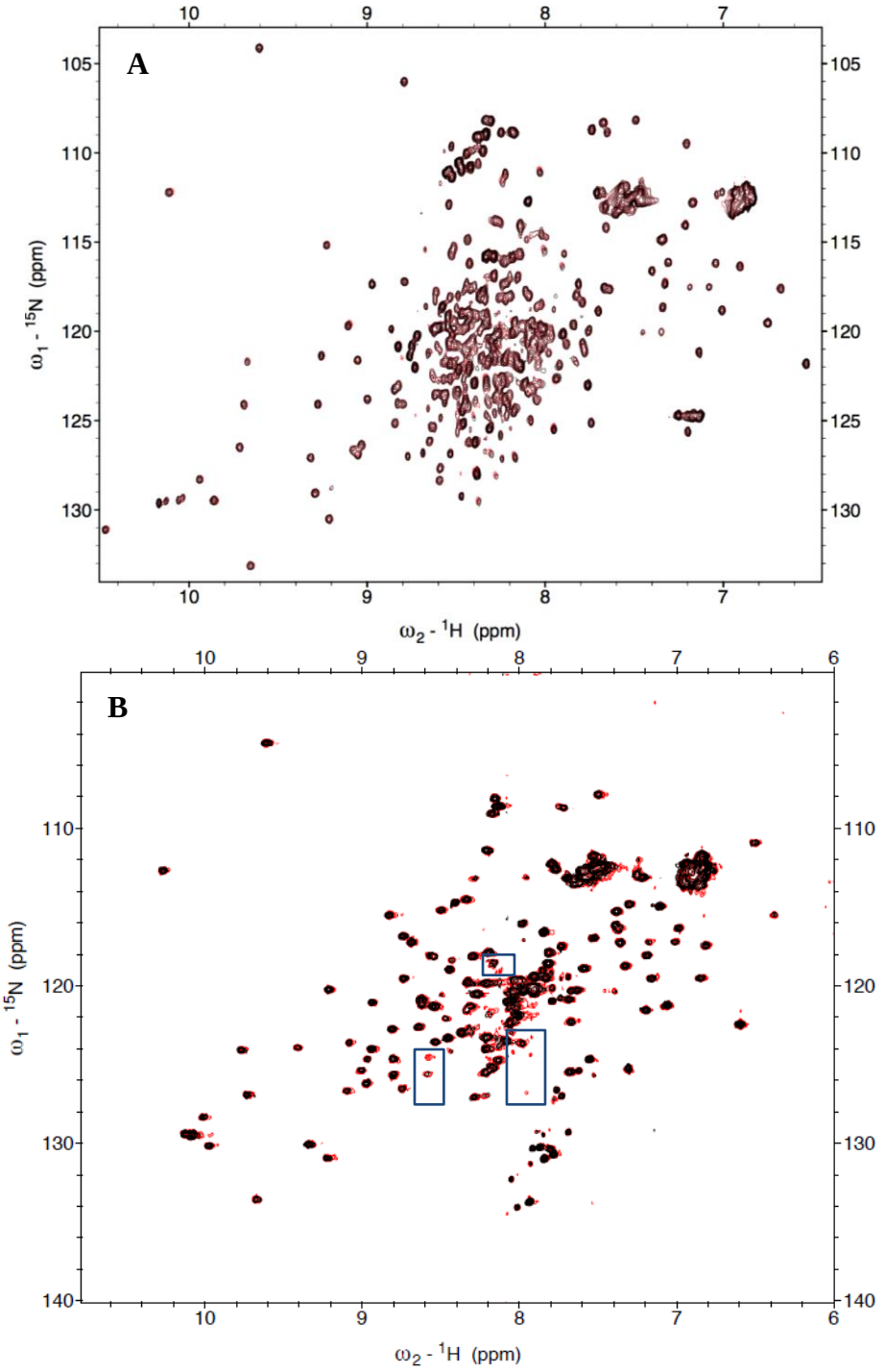

Figure 2.6 ^{1}H-^{15}N HSQC spectra of MMP-8 with NCC. (A) Freshly purified sample of 0.3 mM ^{15}N MMP-8 in 10 mM Tris base, 7.4 mM sodium acetate, 5 mM $CaCl_2$, 20 µM $ZnCl_2$, pH 3.0 (black) did not interact with 4:1 excess NCC to MMP-8 (red). No spectral perturbations were seen between the two spectra. (B) Freshly purified sample of 0.3 mM ^{15}N MMP-8 in 50 mM Tris-HCl, 60 mM NaCl, pH 8.5 (black) showed protein interaction with 2:1 excess NCC to MMP-8 (red). The presence of new and increased intensity peaks suggests protein-inhibitor interaction (boxed).

is possible that more extensive changes are induced upon binding NCC but that the effects are not observable using this experimental approach.

2.3.4 Stability Studies

The stability of MMP-8 was analyzed by collecting 2D NMR data at various time points. For the stability studies, HSQC experiments were collected on a sample of 0.3 mM ^{15}N MMP-8 in 50 mM Tris-HCl, 60 mM NaCl, pH 8.5, at 16 h, 24 h, 40 h, 64 h, 7.5 d, and 17 d time points. MMP-8 stability also was investigated in the presence of NCC. HSQC experiments were collected on a sample of 3.0 mM ^{15}N MMP-8, 0.6 mM NCC at the same buffer conditions and time points as the MMP-8 only sample. The overlay of ^{1}H-^{15}N HSQC spectra show the development of new peaks in the region between 7.5-8.2 ppm in the ^{1}H dimension and 124-135 ppm in the ^{15}N dimension for both the MMP-8 only sample (Figure 2.7A) and MMP-8 plus NCC sample (Figure 2.7B). Comparison of the spectra between MMP-8 and MMP-8 with NCC inhibition at 17 days shows the presence of new, sharp peaks in the upper region of the spectra when NCC is not present (Figure 2.8). These peaks likely represent smaller molecular weight fragments and/or disordered portions of the protein that result from proteolytic activity of the enzyme. If NCC is inhibiting MMP-8 while it is interacting with the protein, it is possible that in the absence of inhibitor, the protein-only sample is experiencing greater autoproteolysis.

Samples were analyzed using SDS-PAGE to assess the extent of degradation and the difference in fragment formation between the samples with longer incubation times. A SDS-PAGE gel of the samples at the 17 day time point indicates that MMP-8 is still degrading while interacting with NCC (Figure 2.9). Immediately following purification (0 days), initial MMP-8 sample has a molecular weight (MW) of approximately 35 kDa which is consistent with the actual MW of 35,105 Da (lane 2). The protein-only sample (lane 3) and the protein sample with

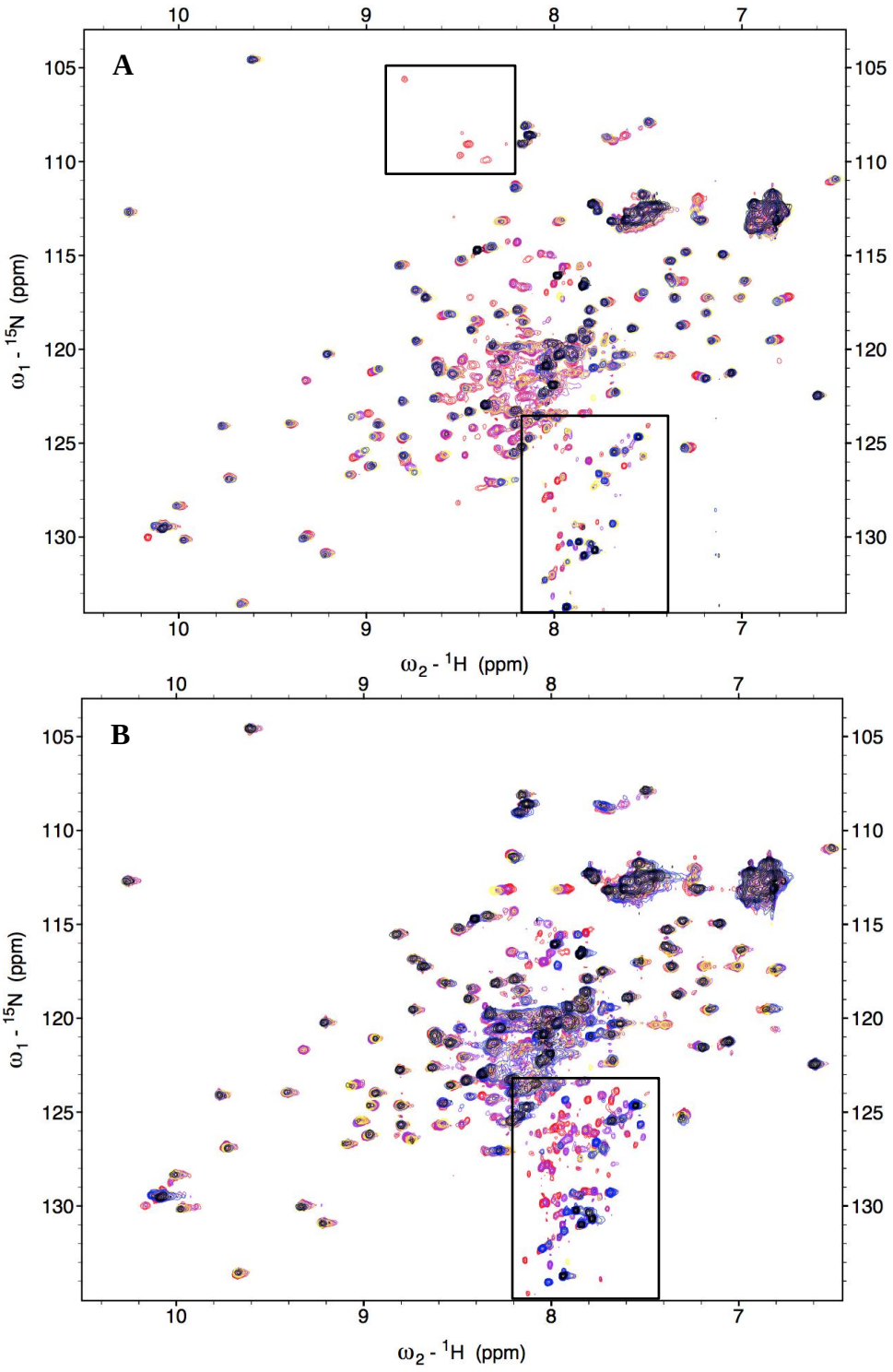

Figure 2.7 ^{1}H-^{15}N HSQC spectra of MMP-8 stability with and without NCC. Sample of 0.3 mM MMP-8 in 50 mM Tris-HCl, 60 mM NaCl, pH 8.5, 0 min (black), 24 h (blue), 64 h (yellow), 7.5 d (purple), and 17 d (red) at room temperature shown. (A) With time, MMP-8 only sample develops extra peaks as protein degrades (boxed). (B) The spectra of 2:1 NCC to MMP-8 sample show more peaks forming as MMP-8 undergoes degradation (boxed).

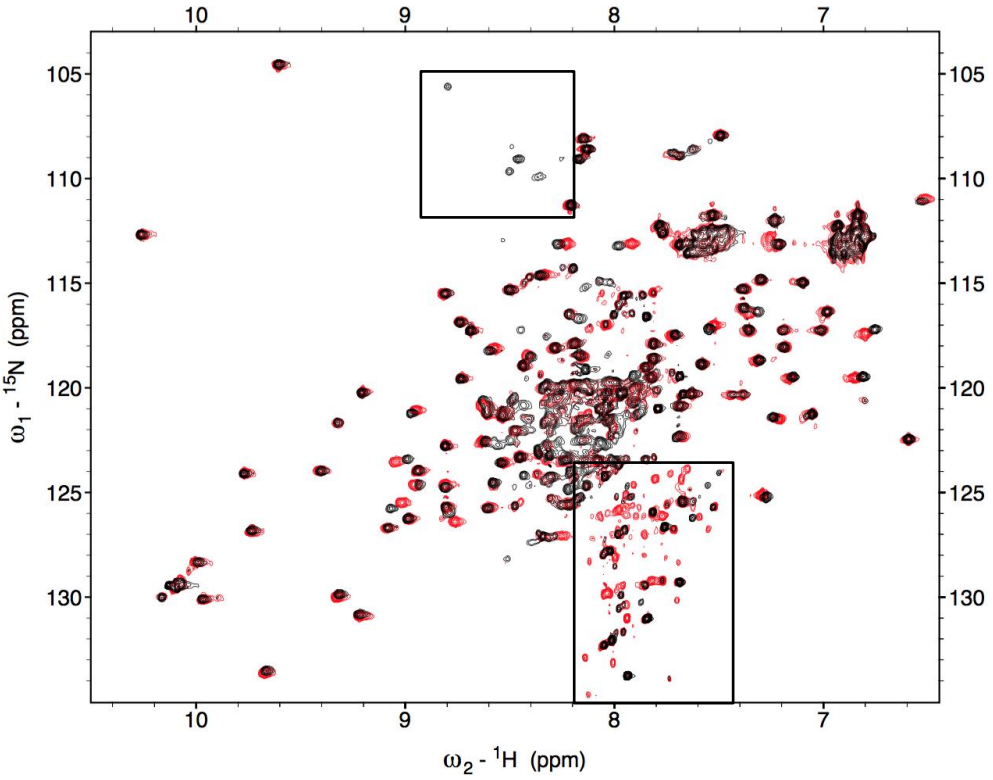

Figure 2.8 ^{1}H-^{15}N HSQC spectra of MMP-8 stability comparison after 17 days. Sample of 0.3 mM MMP-8 in 50 mM Tris-HCl, 60 mM NaCl, pH 8.5, 17 days at room temperature shown. MMP-8 only sample (black) and the 2:1 NCC to MMP-8 sample (red) develops extra peaks, unique to each sample, as the protein degrades (boxed).

NCC (lane 4) at 17 days have faint bands at 35 kDa, indicating loss of most of the intact MMP-8. However, comparison of lanes 3 and 4 shows the presence of different bands in each lane, and thus unique protein fragments, at lower MWs. The two bands around 12 kDa in lane 3 are shifted to slightly higher MWs in lane 4, and lane 4 also

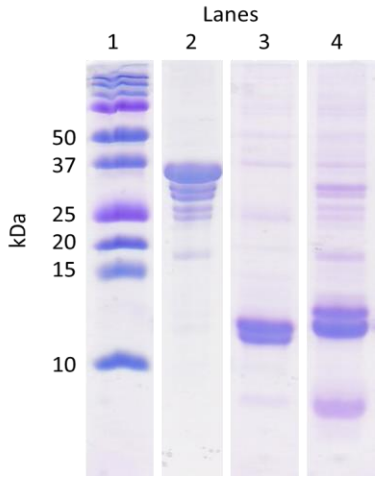

Figure 2.9 Coomassie stained SDS-PAGE gel of MMP-8 stability samples. (Lane 1) molecular weight ladder, (lane 2) 0 days post-purification, (lane 3) 17 days post-purification without NCC, (lane 4) 17 days post-purification with NCC shown. Post-purification MMP-8 samples were kept at room temperature.

has a darker band around 8 kDa. This comparison suggests that the protein degradation pattern may be different when NCC is present. The presence of higher MW bands and a more intense band around 8 kDa suggests that NCC may be maintaining larger protein fragments, and the fragmentation of MMP-8 may be occurring slightly faster in the absence of NCC. Because of the high concentration of MMP-8 used in these assays, the fragments generated were attributed to autoproteolytic activity, but it should be noted that the samples were generated using a simple one-step purification protocol and it cannot be ruled out that contaminating host cell proteins may be present that could contribute to proteolytic degradation.

2.3.5 Temperature Titrations

Temperature optimization for NMR experiments was tested at 20, 25, 30, and 35 ^{o}C with 0.3 mM ^{15}N MMP-8, 0.6 mM NCC, 50 mM Tris-HCl, 60 mM NaCl, pH 8.5 (Figure 2.10A). Other sample condition optimizations were carried out at 25 ^{o}C, but small spectral improvements with changes in temperature would improve data collected during 3D NMR experiments. Lowering the NMR temperature to 20 ^{o}C resulted in decreased resolution in the center of the spectra (Figure 2.10B). An increase in the temperature to 30 ^{o}C yielded better resolution, and the data quality was comparable between the 30 and 35 ^{o}C ^{1}H-^{15}N HSQC experiments (Figure 2.10C).

2.3.6 3D NMR Experiments

To determine the NMR assignment data for MMP-8, the 3D CBCA(CO)NH and HNCACB experiments were collected at 1.0 mM ^{15}N-^{13}C MMP-8 plus bound NCC, 50 mM Tris-HCl, 60 mM NaCl, pH 8.5. The sample used for the 3D experiments was at pH 8.5 to allow for MMP-8 interaction with NCC. At an enzyme concentration of 1.0 mM and above, self-association of the protein was observed, and the observable peaks in the 2D experiments shifted

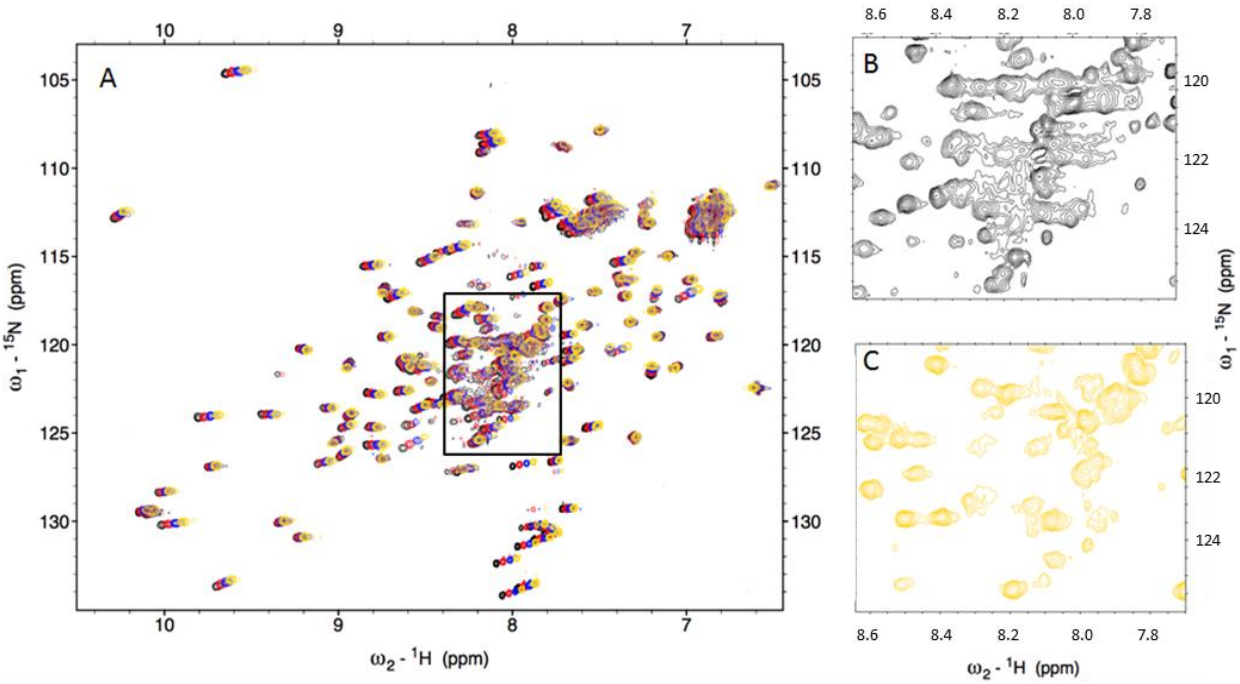

Figure 2.10 ^{1}H-^{15}N HSQC spectra of MMP-8 temperature. Sample of 0.3 mM MMP-8, 0.6 mM NCC in 50 mM Tris-HCl, 60 mM NaCl, pH 8.5, 20 ^{o}C (black), 25 ^{o}C (red), 30 ^{o}C (blue), and 35 ^{o}C (yellow) shown. With increasing temperature, the resolution improves in the central region of the spectra (boxed). Zoomed in spectra of 20 ^{o}C (B) and 35 ^{o}C (C) show improved resolution at higher temperature in the boxed region.

toward the center of the spectrum. Dilution of the sample was slow to reverse the MMP-8 self-association. Concentrating the sample after incubation of a 0.3 mM MMP-8 sample with 0.6 mM NCC prevented protein aggregation, so the 3D experiments were collected on samples containing NCC. The compression of the 3D data sets onto the ^{1}H and ^{15}N axes should display peaks in the same ^{1}H and ^{15}N chemical shifts as the HSQC spectrum (Figure 2.11). In the CBCA(CO)NH, the peaks are concentrated in the center, and most of the outer, structured peaks are missing (Figure 2.12). For each amino acid, the strip plot of the CBCA(CO)NH 3D data should display the two peaks that correspond to the Cα and Cβ of the preceding amino acid (Figure 2.13). Several of the strips are missing the Cα and Cβ peaks which means these

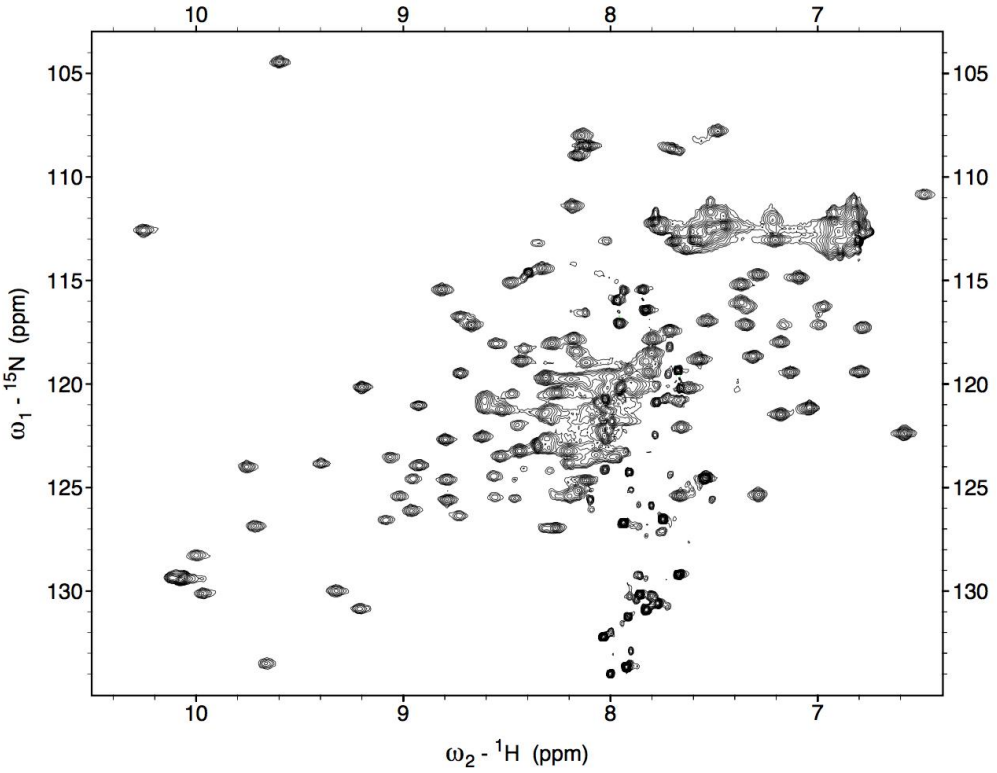

Figure 2.11 ^{1}H-^{15}N HSQC spectra of MMP-8 for peak assignments. Sample of 1.0 mM MMP-8 plus NCC in 50 mM Tris-HCl, 60 mM NaCl, pH 8.5. This spectrum was used for referencing the data from the 3D NMR experiments.

resonances are not detected in the experiment or the strips have more than two peaks and are difficult to interpret due to overlap of the data.

The compression of the HNCACB 3D data onto the ^{1}H-^{15}N plane also shows missing peaks and peaks with reduced intensity in the outer, structured regions of the spectra (Figure 2.14). For this experiment, each HN should have four associated peaks that correspond to the Cα and Cβ of the same amino acid and of the preceding residue. This is represented in the strip plot for each amino acid. Only 25% of the peaks in the HSQC have four peaks in their strip plots, and connectivity to either the preceding or following amino acid in the protein sequence could not be made for many of those peaks (Figure 2.15). Another challenge with this data set is the absence of one or more of the four expected peaks for the Cα and Cβ atoms in individual strips from the

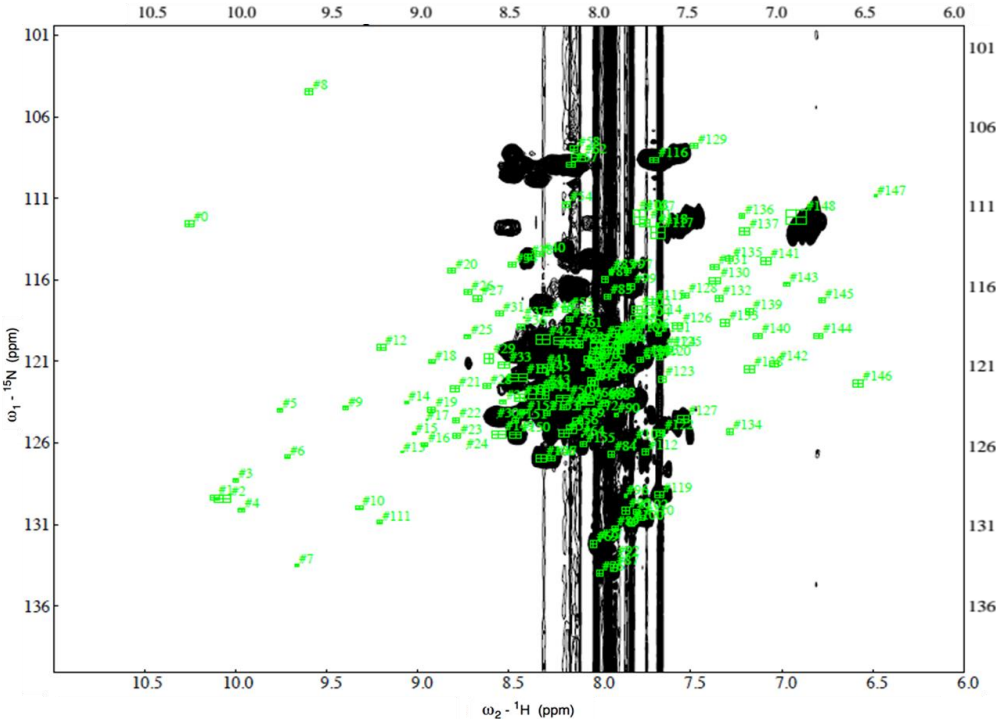

Figure 2.12 CBCA(CO)NH spectra of MMP-8. 2D ^{1}H-^{15}N plane of 3D data from the CBCA(CO)NH experiment for a sample of 1.0 mM MMP-8 + NCC in 50 mM Tris-HCl, 60 mM NaCl, pH 8.5 shown. The numbers, which are referenced to the ^{1}H-^{15}N HSQC spectra, indicate where missing peaks in this data set should be located in the CBCA(CO)NH spectrum.

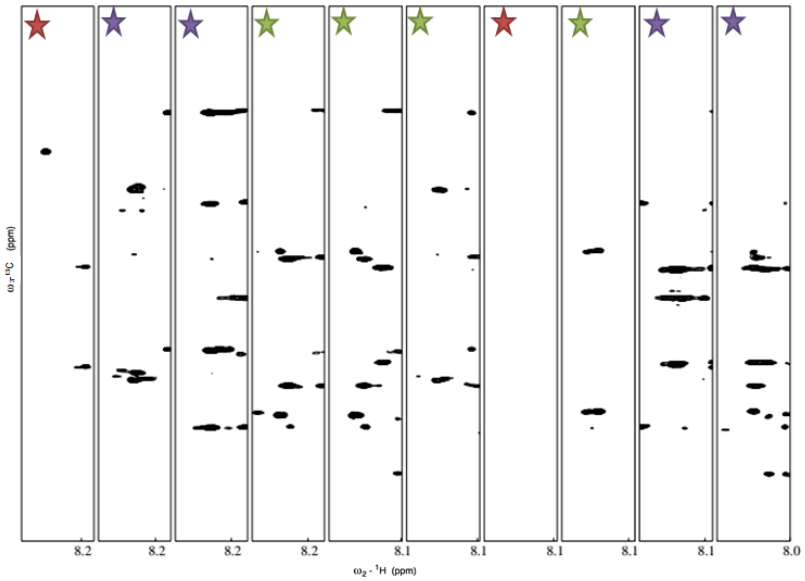

Figure 2.13 Example strip plot of CBCA(CO)NH data from MMP-8. Sample of 1.0 mM MMP-8 + NCC in 50 mM Tris-HCl, 60 mM NaCl, pH 8.5, CBCA(CO)NH strips with good data, showing 1 Cα and 1 Cβ peak, (green), missing Cα and Cβ peaks (red), and overlapping data (purple).

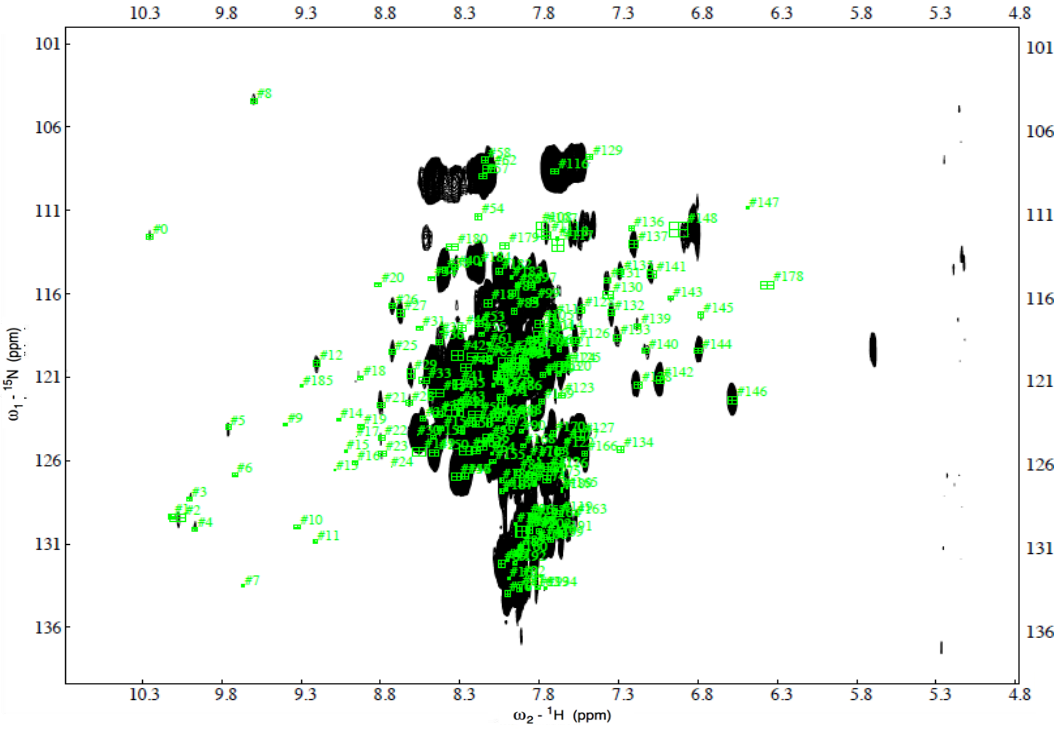

Figure 2.14 HNCACB data from MMP-8. 2D ^{1}H-^{15}N plane of 3D data from HNCACB experiment for a sample of 1.0 mM MMP-8 + NCC in 50 mM Tris-HCl, 60 mM NaCl, pH 8.5 shown. The numbers, which are referenced to the ^{1}H-^{15}N HSQC spectra, indicate where peaks should be located in the HNCACB spectrum.

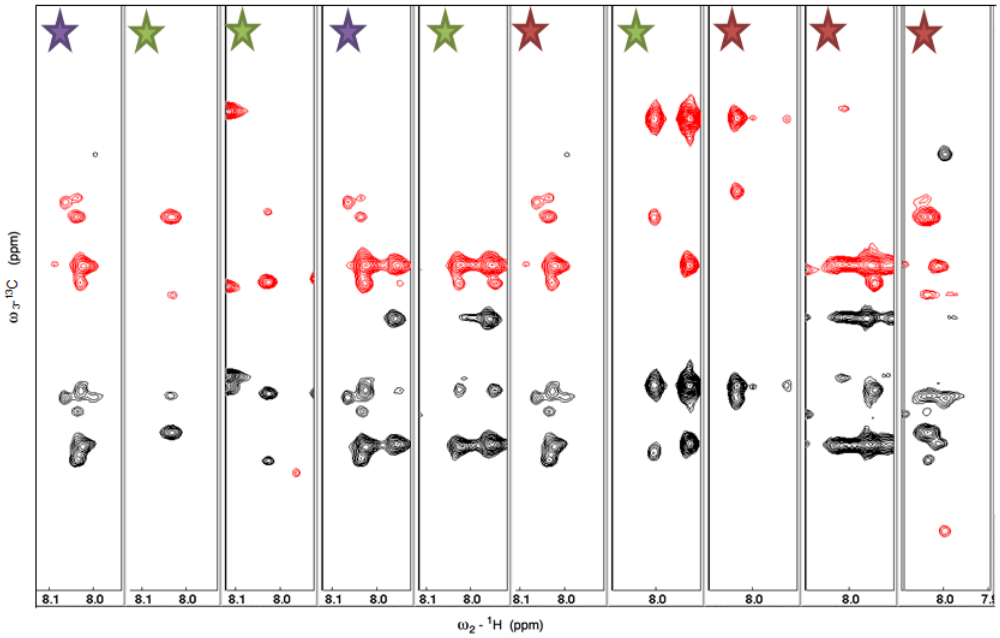

Figure 2.15 Example strip plot of HNCACB data from MMP-8. Sample of 1.0 mM MMP-8 + NCC in 50 mM Tris-HCl, 60 mM NaCl, pH 8.5, HNCACB strips with good data, showing 2 Cα and 2 Cβ peaks, (green), missing Cα and Cβ peaks (red), and overlapping data (purple).

3D data set. Without having all four peaks, it is impossible to derive connectivity between the amino acids in the polypeptide chain. The data from the HNCACB experiment was even less complete, and resonances for only 15% of the Trx MMP-8 fusion amino acid residues were present in the spectrum. Because these experiments produced only a very small fraction of the peaks observed in the best 2D HSQC, and this represented only 60% of the protein at most, it was concluded that even partial NMR assignments of MMP-8 could not be made under the conditions chosen based on the 2D range-finding HSQC experiments.

2.4 DISCUSSION

Condition optimization experiments for MMP-8 provide interesting information about the protein's behavior in different chemical environments, its stability, and protein-inhibitor interactions. The structure of MMP-8 was improved at lower pH, as observed with better peak resolution in the ^{1}H-^{15}N HSQC spectra. Of the conditions tested, pH 3.0 with excess Ca^{2+} and Zn^{2+} ions resulted in the best spectral resolution in the ^{1}H-^{15}N HSQC compared to samples at higher pH. The metal ions do not bind covalently to MMP-8 and follow the principle of equilibrium. When MMP-8 is purified, metal ions occupy the metal binding sites, but during purification, excess ions are removed to some extent. With time, the equilibrium of bound vs free ions shifts since few to no ions occupy the surrounding environment initially. At low pH, the binding affinity of the metals is lower due to competition for binding with increased protons in the sample solution. Without the addition of excess metal ions, exchange occurs and the average of the protein signal with and without ligands bound is measured. When excess Ca^{2+} and Zn^{2+} ions are added, the protein obtains a more rigid and less flexible structure since the equilibrium shifts toward bound metal ions.

The Ca^{2+} and Zn^{2+} ions in MMPs are important for structure and enzymatic function [25]. However, little research has focused on the mechanisms of the structural and functional roles of the metal ions in MMP-8. Functional MMP-8 coordinates one catalytic Zn^{2+} ion, an additional structural Zn^{2+} ion, and two structural Ca^{2+} ions [11]. By using NMR alone, it is difficult to say which ion(s) were lost through dialysis of MMP-8 at low pH and which are important for maintaining tertiary structure. From the low pH dialysis studies, it was determined that Zn^{2+} ions are lost during purification to an appreciable extent and that zinc is more important for enzyme structure compared to the Ca^{2+} ions. From the current data set, it cannot be determined whether one or both of the Zn^{2+} ions are removed by dialysis. The affinity of MMP-8 for the individual Ca^{2+} and Zn^{2+} ions and the mechanism of the ions' functions, enzymatic action and/or structural roles, are currently not established.

In a study with MMP-26, which also has two Ca^{2+} ions, sequence alignment with other MMPs and crystal structure analysis indicated the presence of both a low and a high affinity Ca^{2+} ion. The low affinity Ca^{2+} ion (120 μM dissociation constant) was more easily dialyzed out of the protein, caused structural changes at the catalytic site, which is important for regulation of enzymatic activity, and resulted in a decrease of catalytic activity (Figure 2.16) [22]. Additionally, the removal of the high-affinity Ca^{2+} ion (62.9 nM dissociation constant), which is important for protein folding and initial stabilization of the tertiary structure, did not affect the tertiary protein structure.

The mechanisms and functions of the metal ions do vary between the MMPs, so it is not possible to predict accurately the role of the metal ions in MMP-8 from the study with MMP-26. Most of the residues that do coordinate the metal ions, described below, are conserved in all MMPs including MMP-8, so it is reasonable to expect the ions would serve similar functions in

MMP-8 [12]. Comparison of MMP-8 and MMP-26 structures indicate similarities, so the Ca^{2+} ions may have similar roles in MMP-8. Based on the binding constant, by analogy the low-affinity site would be empty but the high-affinity site would likely remain occupied with calcium following purification of MMP-8 in this study. Future studies of MMP-8 using a series of mutants to investigate the effects of metal chelators, including activity assays and structural analyses such as circular dichroism (CD) spectroscopy, may contribute more information about which metal ions are important for structure and function and their affinities to MMP-8.

Figure 2.16 MMP-26 structure comparison. The light gray ribbon shows MMP-26 structure in the presence of low affinity Ca^{2+} ions, and the dark gray ribbon shows the structural changes when these ions are removed. The light gray spheres, C2 and C3, indicate possible low affinity Ca^{2+} ions, where C2 most likely is not a Ca^{2+} ion binding location. The dark gray sphere, C1, indicate the high-affinity Ca^{2+} ion. The small light and dark gray spheres represent the Zn ions in the presence and absence of low affinity Ca^{2+} ions, respectively. Reproduced with permission from, *Biochem. J.* 403, 31–42 © 2007 Biochemical Society [22].

Without knowing which ions are removed in dialysis and if they impact the tertiary structure, it is possible that the removal of the catalytic Zn^{2+} ion resulted in loss of tetrahedral ligation, and thus the loss of structure was observed in the ^{1}H-^{15}N HSQC spectra. The catalytic Zn^{2+} ion of MMP-8 is liganded by the imidazole nitrogen atoms from three histidine residues (Figure 1.3) [26]. The other Zn^{2+} ion, thought to maintain tertiary structure, is also tetrahedrally coordinated by three histidine residues and an aspartic acid residue [12]. One of the Ca^{2+} ions has octahedral coordination involving two aspartic acid residues, one glutamic acid residue, one glycine residue, and the backbone of one

isoleucine residue. The other Ca^{2+} ion is coordinated between two glycine residues and two aspartic acid residues, as determined in the 2OY4 uninhibited MMP-8 crystal structure in the Protein Data Bank [27]. At low pH, the nitrogen of the histidine residues and the oxygen atoms of the glutamic acid and aspartic acid residues become protonated, and the protons reduce the charge of these moieties and consequently the affinity of the Zn^{2+} and Ca^{2+} ions for the protein binding sites. With low pH dialysis, the metal ions ultimately are removed from their coordination sites and replaced with hydrogen atoms, which removes the structural interaction between distal amino acids and results in loss of tertiary structure. The Ca^{2+} ion described above is within a compact loop structure that is thought to stabilize the whole domain, so loss of this ion would result in unfolding of MMP-8 [12]. As such, the HSQC spectra of the purified MMP-8 sample and MMP-8 with excess calcium added indicate that this Ca^{2+} ion largely remains bound during purification of the enzyme. The addition of excess metal ions helped to saturate the binding sites and stabilize the protein structure by driving the equilibrium of the metals to the liganded state, thereby improving the NMR spectrum by reducing conformational exchange.

Further investigations of MMP-8 at low pH were studied with the addition of inhibitors. Interactions between NNGH and MMP-8 were unable to be determined because DMSO, the solvent for NNGH, greatly changed the structure of MMP-8. DMSO denatures a protein, disrupting secondary structure, by breaking hydrogen bonds, hydrophobic interactions, and salt bridges [28]. Because of this, the water-soluble inhibitor NCC was used in an effort to study the mechanism of inhibition of MMP-8. Testing of the NCC peptide by previous group members has indicated that NCC will coordinate Zn^{2+} ions. When NCC was previously incubated with and bound to a metal, it did not interact with MMP-8, which further suggests that NCC interacts with the Zn^{2+} ion in the MMP-8 active site [15]. In previous studies, it is evident that NCC interacts

with MMP-8 [15, 16]. However, as expected from studies involving other divalent cations, NCC did not interact with MMP-8 at low pH. Previous studies demonstrate that NCC releases Ni^{2+} ions at neutral pH. The exact pH profile for NCC binding to Zn^{2+} ions has not been determined experimentally, but it is known that pH 3.0 is a low enough pH for NCC to not bind and to release bound Zn^{2+} ions.

Because NCC did not interact with MMP-8 at low pH, the sample was studied further at basic pH. Each of the amino acids composing a protein has a distinct charge state and the protein has an isoelectric point derived from its unique composition. Adjusting the sample pH can cause protonation or deprotonation of the ionizable side chain moieties, including carboxylic acids, amines, imidazoles, and thiols. Altering the pH of the solution affects the solubility of the protein, decreasing it as the solution approaches the protein's isoelectric point. Changes in pH also can lead to localized or global transitions in protein structure or confirmation [29, 30] and stability of the fold as well. Protonation or deprotonation of a residue causes changes in the electric field surrounding the nuclei involved and neighboring residues [31, 32], which are detectable in the NMR as chemical shift perturbations [33]. All of these possible changes in the chemical environment as an effect of pH, protein folding and ligand interactions, can lead to chemical shift changes in the HSQC spectrum for most nuclei in a protein and may impact spectral resolution.

In investigations at basic pH (8.5), chemical shift changes in the presence of NCC were observed and therefore the site of interaction with MMP-8 could be characterized using this approach. The small perturbations in the ^{1}H-^{15}N HSQC spectrum suggest that the interaction is in one localized area of MMP-8 and most of the protein structure remains unchanged. Due to the metal binding properties of NCC, the peptide is expected to interact directly with the Zn^{2+} ion in

the MMP-8 active site. Based on the NMR data, it must be concluded that the peptide does so without displacing other coordinating ligands or more likely that this critical portion of the enzyme simply is absent from the spectra, preventing the use of perturbation analysis to detect the binding site. What is clear from the present data set, and confirms previous conclusions, is that NCC does not remove metal ions from MMP-8 [15]. It is known that NCC does not bind Ca^{2+}, so any observed changes would be attributable to its interaction with Zn^{2+}. It was established in Tucker *et al.* that NCC binds the Zn^{2+} ion while it remains coordinated by MMP-8 [15]. If the Zn^{2+} ion was removed from the protein during the long incubation period, the tertiary structure would change significantly, and the HSQC spectrum would appear similar to the spectrum in which the metal ions were removed from the protein by dialysis at low pH. Unfortunately our data set was insufficient to characterize the interaction, and more complete 3D data to support peak assignment is needed to confirm how NCC interacts with the Zn^{2+} ion in the MMP-8 active site.

The stability of the MMP-8 protein sample also was a concern because the 3D NMR experiments require the sample to be at or above room temperature for several days. The proteolytic function of MMPs allows for increased autoproteolysis at these temperatures, which makes production of stable proteins difficult [2]. The structure of MMP-8 remains mostly intact upwards of 7 days, which means the sample will be stable enough for the collection of the 3D NMR experiments. However, several new peaks around 7.5-8.2 ppm in the ^{1}H dimension and 124-135 ppm in the ^{15}N dimension in the spectra, both with and without NCC inhibition, develop within a couple days. The presence of new peaks suggests that while the protein chain remains largely intact during this period, MMP-8 structure is deteriorating with time, even within the 4 to 5 day time frame needed for the 3D NMR experiments. Previous studies have indicated that

fragmentation of MMP-8 does not affect protein activity [3]. Comparison of the ^{1}H-^{15}N HSQC of the samples at 17 days shows the presence of several new peaks around 8.3-9.0 ppm in the ^{1}H dimension and 105-110 ppm in the ^{15}N dimension when NCC is not present. It is possible that NCC is preventing some degradation and change in the MMP-8 protein structure that normally occurs without inhibition. Previous studies have shown that in the presence of NCC, MMP-8 activity is reduced, and in the absence of NCC, enzyme activity is retained even after fragmentation [3]. With the structural changes and degradation, it is also possible that NCC is changing the cleavage pathway.

After 17 days at room temperature, the protein sample is significantly degraded from its original band on the SDS-PAGE gel, even in the presence of NCC. From visual analysis of the gel, both samples no longer have the intact protein after 17 days. The remaining bands on the gel are different between the sample with and without NCC, which indicates a differences in fragmentation rate or pattern. SDS-PAGE gels were not run at other time points, so it is difficult to draw conclusions about MMP-8 degradation. Further SDS-PAGE stability studies at additional time points will need to be completed to better understand the rate of MMP-8 degradation and effectiveness of NCC inhibition.

With other metals, NCC has been demonstrated to abstract the metal ion, removing it from the original chelating group and sequestering it in basic solutions. It is possible that the same reaction occurs with zinc but at a greatly reduced rate. If this is happening slowly in the NCC-containing MMP-8 sample, then unfolding of the enzyme should occur.

The peaks that appear in the HSQC of the NCC-containing sample over time correspond to the chemical shift region where sequences lacking stable structure appear. The appearance of these peaks suggests that portions of the protein are being unfolded and losing structure. The fact

that hallmarks of degradation appear in both MMP-8 spectra but differ in the absence and presence of NCC suggest that ultimately the metal ion may be abstracted by the inhibitor. This hypothesis is consistent with all existing data but further investigation would be required to explore this possible mechanism.

Several factors explain reasons for the unsuccessful 3D NMR experiments. The Trx-MMP-8 fusion protein consists of 323 amino acids, which is large for standard 3D NMR studies. Nonetheless, many proteins of this size or larger have been studied successfully using high-resolution solution NMR [34-36]. MMP-8, Trx, and the S-Tag make up 161, 126, and 33 amino acid residues of the fusion protein, respectively. There is a limited window of possible ^{1}H, ^{15}N, and ^{13}C chemical shifts for amino acids based on their chemical environment, so larger proteins may yield overlapping peaks, as more peaks need to fit within the same chemical shift range [37]. Poor resolution in NMR experiments of proteins may also result from non-ideal relaxation pathways. Although the 2D ^{1}H-^{15}N HSQC had good resolution and intensity of peaks, the sensitivity of the experiment and therefore the intensity of peaks inherently decrease with 3D NMR experiments. For 3D data collection, more time is needed for data acquisition, and longer pulse sequences are required [37]. For a 30 min 2D HSQC, 180 points were collected for the ^{15}N dimension, but for a 4.5 day 3D CBCA(CO)NH, 56 and 176 data points were collected for the ^{15}N and ^{13}C dimensions, respectively. With fewer data points for 3D experiments, the signal intensity and resolution will decrease. To help overcome reduced signal intensity, higher MMP-8 concentration samples were used.

Several paths forward are possible to attempt to improve the 3D NMR data quality and allow for protein assignment. Using a deuterated protein would allow for shorter relaxation pathways, which could improve peak resolution and reduce overlap in the data [37]. The

Trx-MMP-8 protein would need to be grown up in *E. coli* in 100% D_2O with deuterated d_6-glucose and labeled with ^{15}N and ^{13}C. This labeling technique is expensive and with the very large number of peaks missing from the 3D data set that appear in the 2D data, this approach is not likely to yield a greatly improved outcome. The HN chemical exchange is likely the biggest problem at basic pH, so using a deuterated protein may not offer the best solution. It is likely that chemical exchange at basic pH and the intermediate time scale of protein dynamics and conformational changes result in data loss. Improvement in solubility of the fusion protein near neutral pH could be altered to allow for collection of data at conditions that allow for better chemical exchange. Another option to test before trying deuteration would be to further investigate better sample conditions. At lower pH (3.0) and with excess Ca^{2+} and Zn^{2+} ions, the HSQC of MMP-8 fusion displayed sharper, better resolved peaks. Conducting the 3D NMR experiments at a low pH and with excess metal ions may result in better 3D data for a greater percentage of the protein sequence. This approach would not, however, provide information about how NCC interacts with MMP-8 because NCC does not interact with the enzyme at low pH, and the excess ions may interfere with NCC binding to the enzyme if it coordinates excess Zn^{2+} ions. If the conditions with low pH and excess ions do allow for improved signals in the 3D NMR experiments, this condition may be useful to investigate MMP-8 interactions with other inhibitors.

Because the main goal of the study was to understand the mechanism of inhibitor interaction with MMP-8, selective labeling of amino acids that are present in and around the MMP-8 active site might allow for identification of the inhibitor binding location. From previous crystal structure data, the active site pocket does consist of a leucine residue, so ILV labeling technique, which labels isoleucine, leucine, and valine methyl groups, could be used to show

perturbations at the active site from inhibitor interactions [38]. In the active site, 3 histidine residues interact with the Zn^{2+} ion, so selective ^{15}N-labeling of Trx-MMP-8 histidine residues would also indicate changes at the active site if inhibitors are interacting with Zn^{2+} [39]. If ILV labeling and selective ^{15}N-labeling techniques were investigated, several mutations in the protein sequence would need to be made individually to identify which labeled peak in the ^{1}H-^{15}N HSQC spectra correspond to the leucine or histidine residues in the MMP-8 active site, and making multiple mutations takes additional time and resources. This approach would require that the inhibitors interact at a site on MMP-8 where ILV methyl labels are present. Even with all these possible future paths, improved and successful data that allows for spectral assignment and/or determination of inhibitor interaction is not a guarantee.

2.5 CONCLUSIONS

In these studies, the structural role of the metal ions of MMP-8 was observed, and a range of sample conditions were investigated to identify a path to 3D NMR data collection to accomplish backbone resonance assignment. Trx-MMP-8 has been shown to interact with the metal binding peptide NCC. Although the backbone assignments were not able to be determined, further insight into the protein-inhibitor interaction was established. From the NMR studies, NCC does interact with MMP-8 in a localized region, most likely interacting with the Zn^{2+} ion in the active site. To further understand the mechanism of inhibitor interaction, alternate protein labeling approaches may prove to be useful.

2.6 REFERENCES

1. Buchwald, P., *Small-molecule protein-protein interaction inhibitors: therapeutic potential in light of molecular size, chemical space, and ligand binding efficiency considerations.* IUBMB Life, 2010. **62**(10): p. 724-31.
2. Koo, H.M., J.H. Kim, I.K. Hwang, S.J. Lee, T.H. Kim, K.H. Rhee, and S.T. Lee, *Refolding of the catalytic and hinge domains of human MT1-mMP expressed in Escherichia coli and its characterization.* Mol Cells, 2002. **13**(1): p. 118-24.
3. McNiff, M.L., E.P. Haynes, N. Dixit, F.P. Gao, and J.S. Laurence, *Thioredoxin fusion construct enables high-yield production of soluble, active matrix metalloproteinase-8 (MMP-8) in Escherichia coli.* Protein Expr Purif, 2016. **122**: p. 64-71.
4. LaVallie, E.R., Z. Lu, E.A. Diblasio-Smith, L.A. Collins-Racie, and J.M. McCoy, *Thioredoxin as a fusion partner for production of soluble recombinant proteins in Escherichia coli.* Methods Enzymol, 2000. **326**: p. 322-40.
5. Skinner, A.L. and J.S. Laurence, *High-field solution NMR spectroscopy as a tool for assessing protein interactions with small molecule ligands.* J Pharm Sci, 2008. **97**(11): p. 4670-95.
6. Levy, G.C. and D.J. Craik, *Recent developments in nuclear magnetic resonance spectroscopy.* Science, 1981. **214**(4518): p. 291-9.
7. Evans, J., *Biomolecular NMR spectroscopy*. 1st ed. 1995.
8. Roberts, G.C., *Applications of NMR in drug discovery.* Drug Discov Today, 2000. **5**(6): p. 230-240.
9. Wishart, D., *NMR spectroscopy and protein structure determination: applications to drug discovery and development.* Curr Pharm Biotechnol, 2005. **6**(2): p. 105-20.
10. Salvatella, X. and E. Giralt, *NMR-based methods and strategies for drug discovery.* Chemical Society Reviews, 2003. **32**(6): p. 365-372.
11. Betz, M., P. Huxley, S.J. Davies, Y. Mushtaq, M. Pieper, H. Tschesche, W. Bode, and F.X. Gomis-Ruth, *1.8-A crystal structure of the catalytic domain of human neutrophil collagenase (matrix metalloproteinase-8) complexed with a peptidomimetic hydroxamate primed-side inhibitor with a distinct selectivity profile.* Eur J Biochem, 1997. **247**(1): p. 356-63.

12. Bode, W., P. Reinemer, R. Huber, T. Kleine, S. Schnierer, and H. Tschesche, *The X-ray crystal structure of the catalytic domain of human neutrophil collagenase inhibited by a substrate analogue reveals the essentials for catalysis and specificity.* The EMBO Journal, 1994. **13**(6): p. 1263-1269.
13. Brandstetter, H., F. Grams, D. Glitz, A. Lang, R. Huber, W. Bode, H.-W. Krell, and R.A. Engh, *The 1.8-Å crystal structure of a matrix metalloproteinase 8-barbiturate inhibitor complex reveals a previously unobserved mechanism for collagenase substrate recognition.* Journal of Biological Chemistry, 2001. **276**(20): p. 17405-17412.
14. Sharma, R., *Enzyme inhibition: Mechanisms and scopes, enzyme inhibition and bioapplications*. 2012: InTech.
15. Tucker, J.K., M.L. McNiff, S.B. Ulapane, P. Spencer, J.S. Laurence, and C.L. Berrie, *Mechanistic investigations of matrix metalloproteinase-8 inhibition by metal abstraction peptide.* Biointerphases, 2016. **11**(2): p. 021006.
16. Dixit, N., J.K. Settle, Q. Ye, C.L. Berrie, P. Spencer, and J.S. Laurence, *Grafting MAP peptide to dental polymer inhibits MMP-8 activity.* J Biomed Mater Res B Appl Biomater, 2015. **103**(2): p. 324-31.
17. Krause, M.E., A.M. Glass, T.A. Jackson, and J.S. Laurence, *MAPping the chiral inversion and structural transformation of a metal-tripeptide complex having Ni-superoxide dismutase activity.* Inorganic Chemistry, 2011. **50**(6): p. 2479-2487.
18. Skinner, A.L. and J.S. Laurence, *1H, 15N, 13C resonance assignments of the reduced and active form of human protein tyrosine phosphatase, PRL-1.* Biomolecular NMR assignments, 2009. **3**(1): p. 61-65.
19. Delaglio, F., S. Grzesiek, G.W. Vuister, G. Zhu, J. Pfeifer, and A. Bax, *NMRPipe: a multidimensional spectral processing system based on UNIX pipes.* J Biomol NMR, 1995. **6**(3): p. 277-93.
20. Goddard, T.D. and D.G. Kneller, *SPARKY*. 2004: University of California, San Francisco.
21. Johnson, B.A. and R.A. Blevins, *NMR View: A computer program for the visualization and analysis of NMR data.* J Biomol NMR, 1994. **4**(5): p. 603-14.

22. Lee, S., Hyun I. Park, and Q.-Xiang A. Sang, *Calcium regulates tertiary structure and enzymatic activity of human endometase/matrilysin-2 and its role in promoting human breast cancer cell invasion.* Biochemical Journal, 2007. **403**(Pt 1): p. 31-42.
23. Muri, E.M.F., M.J. Nieto, R.D. Sindelar, and J.S. Williamson, *Hydroxamic Acids as Pharmacological Agents.* Current Medicinal Chemistry, 2002. **9**(17): p. 1631-1653.
24. Laurence, J.A.S., A.A. Vartia, and M.E. Krause, *Metal abstraction peptide (MAP) tag and associated methods.*, U.S. Patent, Editor. 2012.
25. Visse, R. and H. Nagase, *Matrix metalloproteinases and tissue inhibitors of metalloproteinases: structure, function, and biochemistry.* Circ Res, 2003. **92**(8): p. 827-39.
26. Gomis-Rüth, F.X., *Structural aspects of the metzincin clan of metalloendopeptidases.* Molecular Biotechnology, 2003. **24**(2): p. 157-202.
27. Bertini, I., V. Calderone, M. Fragai, C. Luchinat, M. Maletta, and K.J. Yeo, *Snapshots of the reaction mechanism of matrix metalloproteinases.* Angew Chem Int Ed Engl, 2006. **45**(47): p. 7952-5.
28. Giugliarelli, A., M. Paolantoni, A. Morresi, and P. Sassi, *Denaturation and preservation of globular proteins: The role of DMSO.* The Journal of Physical Chemistry B, 2012. **116**(45): p. 13361-13367.
29. Tomlinson, J.H., V.L. Green, P.J. Baker, and M.P. Williamson, *Structural origins of pH-dependent chemical shifts in the B1 domain of protein G.* Proteins, 2010. **78**(14): p. 3000-16.
30. Wishart, D.S., *Interpreting protein chemical shift data.* Progress in Nuclear Magnetic Resonance Spectroscopy, 2011. **58**(1–2): p. 62-87.
31. Buckingham, A.D., *Chemical shifts in the nuclear magnetic resonance spectra of molecules containing polar groups.* Canadian Journal of Chemistry, 1960. **38**(2): p. 300-307.
32. Kukic, P., D. Farrell, L.P. McIntosh, B. García-Moreno E, K.S. Jensen, Z. Toleikis, K. Teilum, and J.E. Nielsen, *Protein dielectric constants determined from NMR chemical shift perturbations.* Journal of the American Chemical Society, 2013. **135**(45): p. 16968-16976.

33. Ulrich, E.L., H. Akutsu, J.F. Doreleijers, Y. Harano, Y.E. Ioannidis, J. Lin, M. Livny, S. Mading, D. Maziuk, Z. Miller, E. Nakatani, C.F. Schulte, D.E. Tolmie, R. Kent Wenger, H. Yao, and J.L. Markley, *BioMagResBank.* Nucleic Acids Research, 2008. **36**(suppl 1): p. D402-D408.

34. Estrada, D.F., J.S. Laurence, and E.E. Scott, *Substrate-modulated cytochrome P450 17A1 and cytochrome b5 interactions revealed by NMR.* J Biol Chem, 2013. **288**(23): p. 17008-18.

35. Rennella, E., R. Huang, A. Velyvis, and L.E. Kay, *(13)CHD2-CEST NMR spectroscopy provides an avenue for studies of conformational exchange in high molecular weight proteins.* J Biomol NMR, 2015. **63**(2): p. 187-99.

36. Sarma, A.V.S., A. Anbanandam, A. Kelm, R. Mehra-Chaudhary, Y. Wei, P. Qin, Y. Lee, M.V. Berjanskii, J.A. Mick, L.J. Beamer, and S.R. Van Doren, *Solution NMR of a 463-residue phosphohexomutase: Domain 4 mobility, substates, and phosphoryl transfer defect.* Biochemistry, 2012. **51**(3): p. 807-819.

37. Frueh, D.P., A. Goodrich, S. Mishra, and S. Nichols, *NMR methods for structural studies of large monomeric and multimeric proteins.* Current opinion in structural biology, 2013. **23**(5): p. 734-739.

38. Goto, N.K., K.H. Gardner, G.A. Mueller, R.C. Willis, and L.E. Kay, *A robust and cost-effective method for the production of Val, Leu, Ile (delta 1) methyl-protonated 15N-, 13C-, 2H-labeled proteins.* J Biomol NMR, 1999. **13**(4): p. 369-74.

39. Tanio, M., R. Tanaka, T. Tanaka, and T. Kohno, *Amino acid-selective isotope labeling of proteins for nuclear magnetic resonance study: proteins secreted by Brevibacillus choshinensis.* Anal Biochem, 2009. **386**(2): p. 156-60.